PROC. 19th INT. CONF. HIGH ENERGY PHYSICS
TOKYO, 1978

A 3

Inclusive Charged and Neutral Particle Production in High Energy Hadron-Hadron Collisions

G. GIACOMELLI

University of Bologna, IN FN, Sezione di Bologna, Bologna

§1. Introduction

This talk is a summary of 34 experimental papers presented at this conference on inclusive charged and neutral particle production in high energy hadron-hadron collisions. I apologize for not being able to give proper credit to all the authors, and for presenting only a small fraction of the experimental results.

Table I gives a summary of the bubble chamber results (25 papers). It is apparent from the table that many experiments have been performed with incident high energy K* and p beams. The physics subjects studied, relevent to this talk, may be classified as follows:

i) Multiplicities and multiplicity distributions for charged particles, TT°, K°, $A\backslash$ $I\backslash$ A^0 and S~.

ii) Inclusive single particle spectra for outgoing 7 T - , p_{Bl0W9} K°, $A\backslash$ A^0 and S~.

iii) Measurements of the polarization of the A^0 in single inclusive reactions.

Counter experiments (9 papers) may be classified as:

i) Specific experiments to measure single particle spectra (in ^ p , K^p, $p^{\pm}$p collisions producing TT*, K*, $p^{\pm}$ and *JC*° particles).

ii) Survey-type experiments, which measure the particle composition in a secondary beam, with particles produced in p-nuclei collisions. The papers presented concern: (a) the production of TT*, K*, p*, nuclei and antinuclei; (b) upper limits for the production of new particles.

The experimental results have been analyzed in term of several models of particle production: the quark parton model, triple Regge diagrams, exchanges of Regge trajectories, the thermodynamic model, etc.

The quark parton model, originally proposed for hard scattering, is now used in very many papers to interpret the experimental data at low values of p_t and low values of x, where most of the cross section lies. Triple Regge analyses are performed for data at large x-values. The exchange of particles in Reggeized form is used in a number of cases where one can clearly isolate one (or two) dominant Regge trajectory. The thermodynamic model provided extensive numerical predictions of particle yields in high energy p-p and p-nuclei collisions. Most of the beam survey experiments compare their results with these predictions.

These models are sometimes contradictory one with another, while in other cases they complement each other in the sense that one model applies to a certain kinematic region while another model applies to another one.

Finally a word of caution has to be used: as it is discussed extensively in Whitmore's talk,[1] many particles are not produced directly, but come from the decay of several resonances. Thus one has to be careful in applying the above models directly to the production of particles like the pions, most of which (over 70 %) are not produced directly.

§2. Topological Cross Sections and TT° Production

2.1. Charged multiplicities

Several bubble chamber experiments reported data on charged topological cross sections, multiplicities and correlation coefficients. In particular new data come from BEBC exposed to RF separated beams, (K^+p at 70GeV/c,[2] K~p at 70GeV/c[3]) and from the 30" hybrid system at Fermilab exposed to a 147 *GeV/c* nositive beam.[4]

As an example of the new data Fig. 1 shows the topological cross sections of K^+p collisions: the new data-points at 70 and 147 GeV/c complete the experimental picture for this type of interaction, whose features are

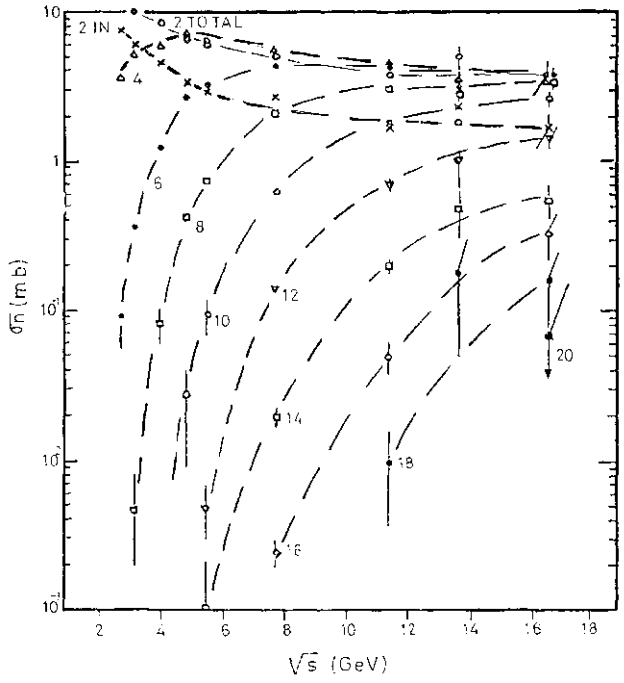

Fig. 1. K⁺p topological cross sections.[2] The new data points presented at this Conference are at 70 and 147 GeV/c.-[4]

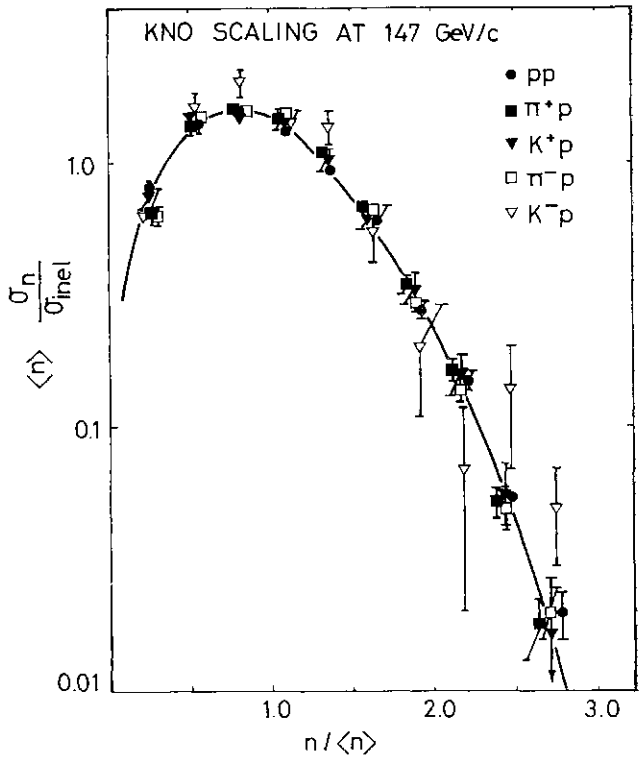

Fig. 2. The KNO scaling function ($\langle\rangle$tfj<7$_{inel}$) plotted *vs* («/<«» for K⁺p, -^p and pp interactions at 147 GeV/c.[4] The solid line is an empirical fit to the data for pp collisions between 50 and 300 GeV/

very similar to pp and r~p interactions.

Figure 2 displays the topological cross sections in the KNO scaling form for K^p, *rc^p*

Table I. Main features of bubble chamber experiments on multiplicities and on inclusive char gee and neutral particle production.

Paper numbers	Institutions	Inter-action	Momentum (GeV/c)	Physics topics studies: Charged Multipl.	*n*°	K_s°	A_9 *A*	Others
547	^EK+Tokyo4-Osaka+ ...	~~p	6	~"			*A*	
474	Bari+Bonn+CERN+ . . .		16					p
141	Dubna—Moscow	~~p	40	*TZ*~, ~⁺	~°			
1065	Caltech—LBL	*TZ'P*	100					
501	Notre D a m e + D u k e .	*rrp*	360		-°	K_s°	*A, A*	
1065	Caltech—LBL	~⁺p	100					
432, 433	Birmingham+CERN + . . .	K"p	8.25				*A* _ *E*~	
25, 828, 1053	URSS+France+CERN	K~p	32			K_s°	*A, A*	*A, A* pol
670	Saclay+RHEL+Paris+ ...	K~p	70	topology	*x*°	K_s°	*A*	
221-225	URSS+France-{-CERN	K⁺p	32	Palow	*x*°		*A, A*	*A* pol
338	Brussels+CERN+ ...	K⁺p	70	topology		K_s^0	*A*	
616	BCCIJMMNOPPRRSTT+..	K⁺p	147	topology				
550	Sendai	pp	0	2 prongs	T T °			
862	Tata+CERN+CdF+ . . .	pp	0.76			K_s°		
436	Tata	pp	3.6			j ^ °	*A, A*	
505	Notre Dame+Tennesee+ . .	pp	4.1		*n*°	K_s°	*A, A*	
727	Amsterdam	pp	12					
302	Alma-Ata-Dubna4- ...	pp	22.4	~~			*A*	
—	SUNY+Tufts+ ...	pp	300		*z*°			
624	KEK+Osaka + Kinki -f -. . .	pp	405				*A, A*	
161	Davies+LBL	pp	405		T T °	K_s^0	*A, A*	
25	Oslo+Stock+ ...	pd	19				^-fragmentation	
768,769	Weizmann+Strasbourg	^⁺d, pd	195	*7:*⁺p_{slow}				

and pp interactions at 147 GeV/c. The five reactions yield points which superimpose closely one on the other and follow closely Slattery's empirical fit[5] to the data for pp collisions between 50 and 300 GeV/c (z=w/<w)>:

$$0(zW3.79z+33.7z^3 -6.64z^5+0.332z^7)e^{-\circ-3^4*} \quad (1)$$

In conclusion KNO scaling seems to hold true for different energies and different types of particles (with only minor problems at the largest *(nKnS)* values).

Many papers report fits of the energy dependence of the total charged multiplicities. The new more accurate data need 3-parameter fits. For example Thome *et al.*[6] have obtained the following fit for pp:

$$</7_{ch}>=(0.88\pm0.10)+(0.44\_b0.05)\ \text{In}\ s +(0.11=b0.006)(\ln\ ^)^2 \quad (2)$$

2.2. Production of TT°

Seven bubble chamber experiments presented results on 7r° multiplicities (see Table I); two of these experiments were performed with the Argonne bubble chamber equipped with a track sensitive target; thus they had a high probability for the conversion of^-rays in contrast to the bare hydrogen bubble chamber where the conversion is rather small. In all experiments, the j'-rays have been assumed to come all from 7T°'s.

I shall only discuss two simple results from these experiments; all other features have the same characteristics.

Figure 3a shows a compilation of TT° multiplicities, plotted versus lab momentum, for $7r^{\pm}p$, K^p and p*p collisions.[7] The main features are the approximate logarithmic rise of the multiplicities and the approximate independence from the type of collisions. These are features which were already observed for the charged multiplicities. In reality the data-points scatter, there are small differences, which could be reduced by using for example the available energy instead of the lab momentum.

A compilation of the correlation coefficient (3) is shown in Fig. 3b.[7] Again one has new information which shows that $f^{\wedge 0}$ is positive, grows with energy and is approximately independent of the type of collisions.

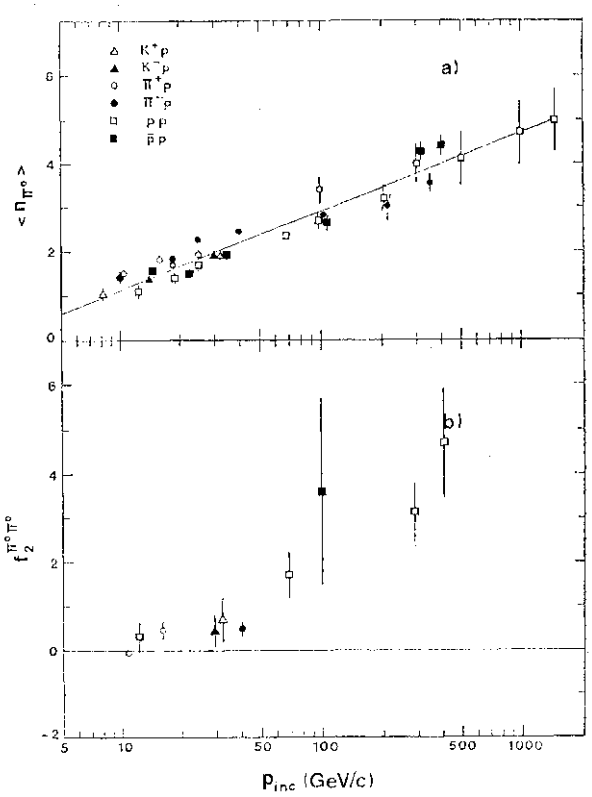

Fig. 3.
(a) Compilaton of *TZ°* multiplicities for TT^P, $K^{\pm}p$, p±p collisions plotted versus lab momentum[7].
(b) $/2^{\pi^0\pi^0}$ correlation coefficients.[7]

§3. Single Particle Inclusive Spectra

3.1. Introduction and notations

Many types of independent variables and of dependencies for the invariant cross sections have been used in the papers presented at this conference:

Energy variable: p_{lab} V s $=E_{cm}$, s (4)

Transverse variable: p_t (5)

Longitudinal variable:

/'Lmax ^max ^ \ F / rL/ (6)

Invariant cross section: (7)

The invariant cross section can only be approximately factorized as done in (7): one should use data at very high energies and factorize in terms of *(p_t, y).* The so-called "seagull effect" prevents a good factorization in terms of *(p_t, x),* while *(p_t, x_n)* improves the

situation. In any case most papers use these approximate factorizations.

The *p^-dependence* is usually taken to be one of these:

exponential $F(p_t)=e^{bpt}$ (8)

gaussian $F(p_t)=e^{bt^2}$ (9)

polynomial $F(P_t)$ (\-pJciy (10)

sum of two exponentials or of two gaussians

At very high energies the exponential dependence is probably the best to fit the data in the $0.1<p_t<1$ GeV/c range. At lower energies, there are differences connected with the type of interaction and on the type of produced particle. In many cases a gaussian is preferred, in particular in the production of resonances[1]; in other cases one needs a sum of two gaussians. The non-directly produced particles distort the spectrum, by enriching the lower /?$_t$-region. No comprehensive analysis in terms of the quark-parton model has been performed until now. In this review we shall not discuss any further the /^-dependence.

Most of the experimental papers have compared their jar-dependence with that suggested by quark-parton models:

$$F(x)=(1-x)^n \quad (11)$$

The ^-values differ in the different models; in the simplest quark recombination model *n* is obtained by counting the minimum number of spectator quarks, /7$_{,,,,,}$:

(12)

For example the following diagram applies to the 7r$^+$—>K$^+$ inclusive reaction:

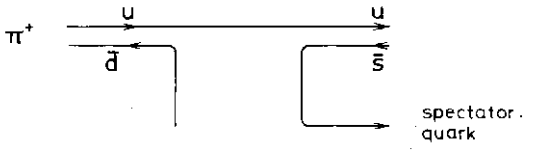

The minimum number of spectator quarks is $_{tf_{ne}ect}$= 1 • Thus one expects *n=2*—1 = 1.

3,2. Inclusive (TT*, X^/^H/J-KTT*, *K*$^{\pm}$, *p±) + X*

Among the extensive counter measurements in pp[8,9] and in (71*, K$^{\pm}$, p)—p[10] collisions presented at this Conference, a small selection of data is presented in Figs. 4, 5, 6.

The inclusive cross sections at fixed p_t plotted versus x or x_R show clearly the leading particle effects for p^p, *TT-^T:*, while the other particles are produced preferentially at

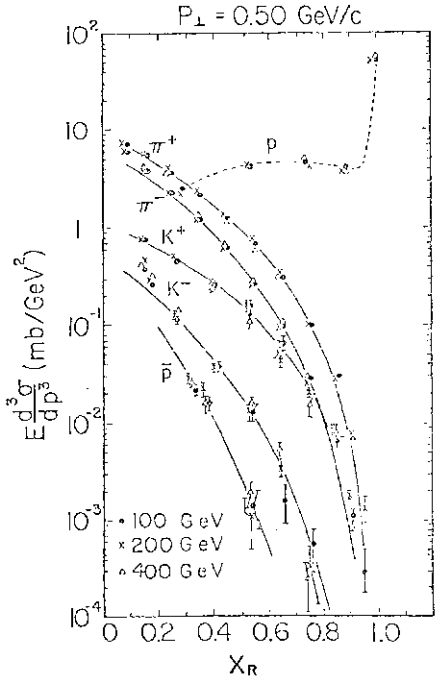

Fig. 4. The invariant cross sections for pp—•(;:', K , p$^+$)+X at /7$_0$ = 400GeV/c and p_t=*0.5* GeV/c plotted *vs* i$_R$.[8] The solid lines are the results of fits to eq. 11.

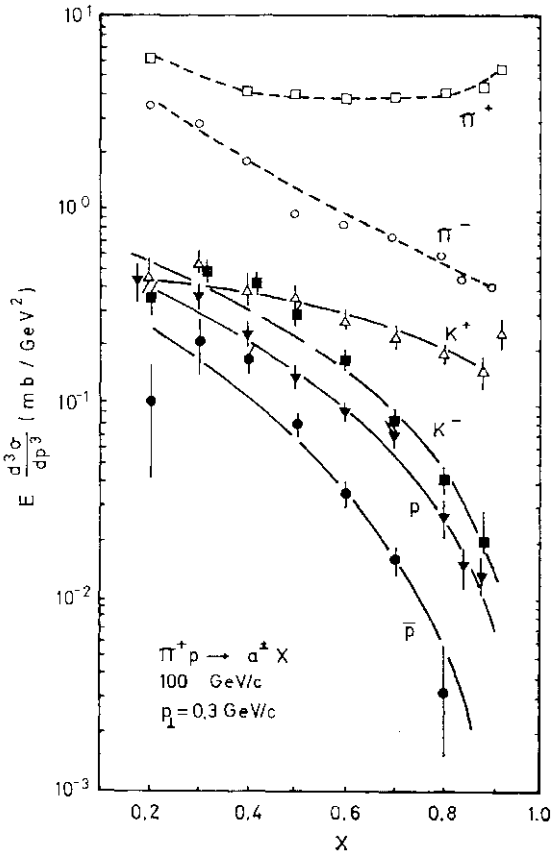

Fig. 5. The invariant cross sections for 7: p- , K^, p-KX at p$_0$-100GeV/c and p_t = *0.3* GeV/r poltted *vs x.*[10]

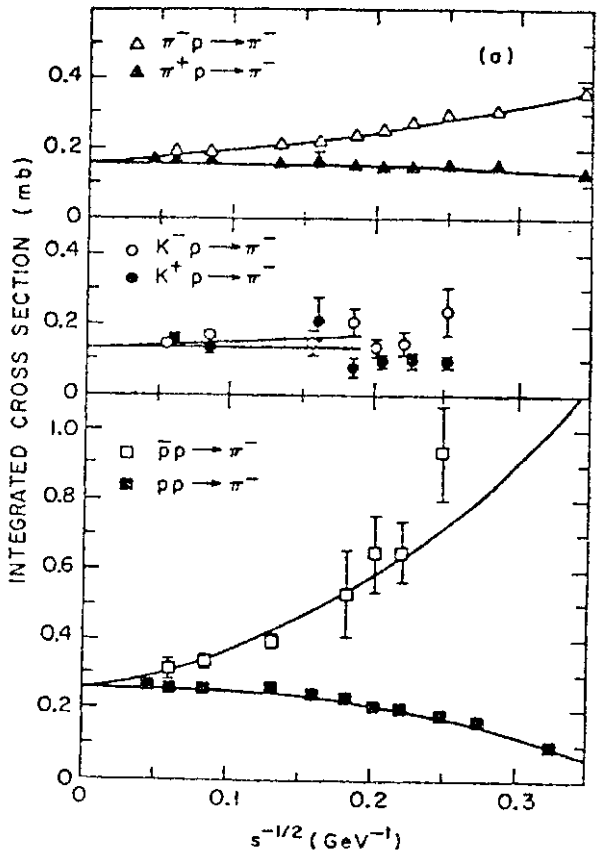

Fig. 6. Cross sections (integrated over a limited angular and momentum region) for the production of T T ~ in (T T ⁺, K⁽ᶜ, p⁺)-proton collisions.[9]

small values of x (or x_n). In Fig. 4 the solid curves represent fits to formula 11, while in Fig. 5 the curves are the predictions of a quark parton model. All fits look reasonable. The values of n obtained are close to the values predicted by the simplest quark-parton model.

The differences from the predictions could be explained as due to contributions from resonances, which are different for each measured particle.

Among the other comparisons with the quark parton model one may recall that the ratio

$$\frac{pp \to 7r^{+} + X}{pp \to :r\sim - \mathbf{I}\ X} \qquad (13)$$

is predicted to become 5 as x->l (the helicity of the fast quark for should be the same as that of the proton). This prediction is in good agreement with the experimental data.[8 1 0]

It may be thus be concluded that quark exchange or annihilation is a dominant process. This is considered by some physicists as surprising since the theoretical motivations for applying quark ideas are well justified only for large-/?, scattering.

At low values of *s* there are many effects, which disappear as s increases, thus yielding many regularities. For example Fig. 6 shows the cross sections for the production of *N~* in 7r⁺p, K⁺p and p⁺p collisions. As *s-^CO* the cross sections for ^-production in *N⁺p* and *7T~p* collisions tend to become equal. The approach to such limit was parametrized in the form[9]

$$Ao = A + Bs\sim^{1\ 2} + Cs\sim^{1} \qquad (14)$$

with *A, B, C* differing for any pair of particles colliding.

3.3. *Inclusive* ***n^p*** **7T° + *X*,** ***n p*** **-» 7r° +** ***all neutrals***

Only a few of the results from a counter experiment on these processes are shown in Figs. 7 and 8.[11,12] The data were interpreted in terms of a Triple-Regge formalism (Fig. 9), which yields the following formulae:

$$\text{tftotOr P}\sim\wedge^{a}\wedge \text{ neutrals}) = A\ s^{n\ \ 1} \qquad (15)$$

$$d^{2}a/dtdx\text{-}F(t)(\backslash\text{-}xr^{i0}\wedge^{2}\wedge\wedge$$

.other trajectories,
^exclusive states, etc. (16)

for $7r^{+}r>\text{-}+7r^{\circ}+X$

$$a(0)\sim a_{p}(0)\sim 1 \qquad (17)$$

for ;r~p->7r°+all neutrals

$$a(0)\sim a_{eff}(0) \qquad (18)$$

The fit of the total neutral cross section, Fig. 7, to eq. 15 yields an effective a=0.08:±: 0.2. Fits of the differential cross sections to eq. 16 yielded good results for x>0.6.

Figure 8 shows that the dominant contribution to the differential cross section is due to the ***OPV*** triple Regge diagram (Fig. 9a).

Table II. Results of the fits of the x-dependence to eq. II.[8] The table gives the w-values fitted; those computed from eq. 12 are given in parenthesis.

	- +	7 1 -	K⁺	K"	p	p
400GeVpp	3.2 (3)	4.0 (3)	2.9(3)	5.0(7)	—	7.6(9)
100GeV7r⁺p	—	—	1.4(1)	2.1(5)	2.2(3)	2.7 (3)

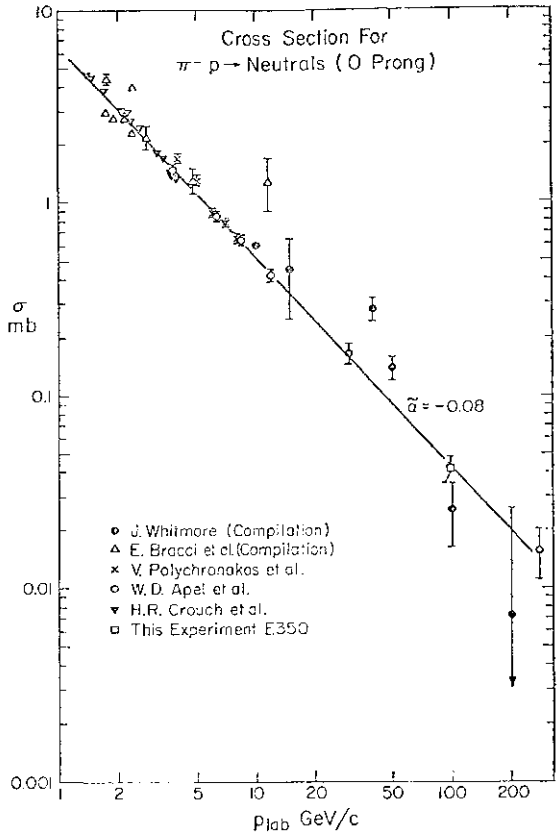

Fig. 7. A compilation of data on ^"p->(neutrals). The solid line is a fit to $o = As^{\alpha}v^{\sim 1}$ with $a\text{-}_{p} = -0.08$.[12]

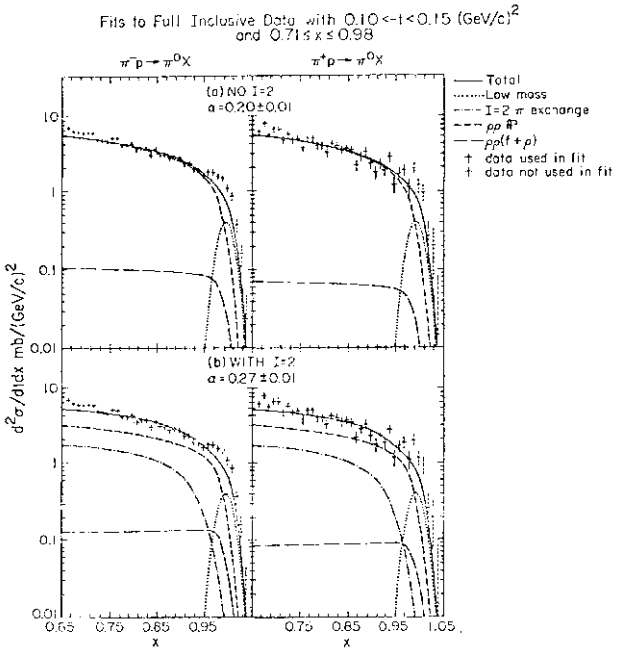

Fig. 8. $d^{2}\boldsymbol{a}/dt\ dx$ *(^p-**tr**^+X)* at 100 GeY/c and O.K—/<0.15 (GeV/c)² plotted *vs x.* The curves represent fits of the and *rrp* data to a Triple-Regge formula including *1=2* terms.[11]

Similar good fits were obtained for the reaction 7r~p->7r°+all neutrals using the basic

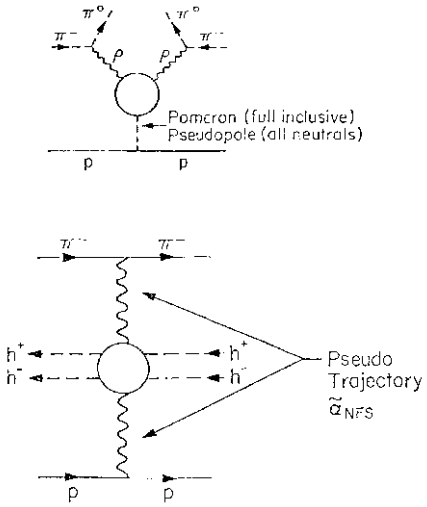

Fig. 9. The simplest Triple Regge diagrams for: (a) ^"p-^7r°+X with *ppv* and (b) for -~p->;r°+all neutrals.

diagram of Fig. 9b. In particular triple Regge dominance is evident from the change in slope of the x-distributions when changing $p_{\perp}$.

From the full inclusive fits the authors obtained the ^-trajectory up to $-1 = 4$ (GeV/c)². Below 1 (Gev/c)² this trajectory is in qualitative agreement from that determined from other methods *(a(j>)* decreases with increasing *—t),* while above 1 (GeV/c)² the trajectory flattens off.

It may be concluded that the interpretation of the extensive measurements of TT° production for *x<0.6* confirms the validity of the Triple Regge formalism in this kinematic region.

3.4. Inclusive K~p-»(K\ A\ I \ A°)+X

The energy dependence of the cross sections for the production of neutral strange particles in K~p interactions is given in Fig. 10: *a(A°+I°)* is approximately constant, slowly increases, while <*J(A°)* increases very fast.

Figures 11 and 12 show compilations of the x-dependence for A^{0} production and for the *A°* polarization in K~p collisions.[13,14] *F(x)* is largest for negative values of *x;* the polarization is zero for *x<0* and negative for x>0. The energy dependence of *P(A°)* is very weak.

These features may be explained qualitatively and quantitatively in terms of the exchanges of Regge trajectories: K, K* exchanges for x<0 and baryon exchanges for x>0. In the forward region P_{A0} and $[F(x)]_{A}o$ can also

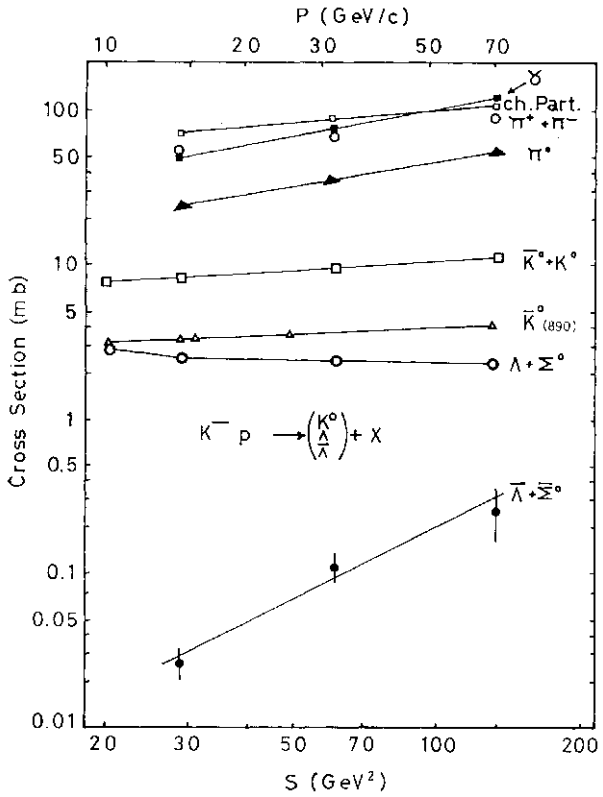

Fig. 10. Energy dependence of K p-^(K°, A^{o}, *1°*, /i°)+X inclusive cross sections.[13]

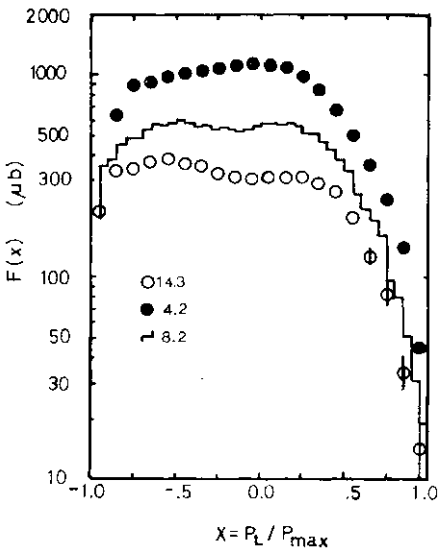

Fig. 11. Invariant cross sections for K p-»(/l°+ *I°)+X* at 4.2, 8.25, 14.3 and 32 GeV/c.[13]

explained by the triple Regge formalism.

3.5. 7v-p-+(K°, A°+2°, A°)+X

The main features of these reactions are shown in Figs. 13, 14 and 15.[15,16]

The multiplicities <X°>, </l°>, <,4°>, increase with energy as In *s* or more (Fig. 13).

The rapidity distributions at 360 GeV/c, *F=F(y)*, show that the K°_{s} are peaked at

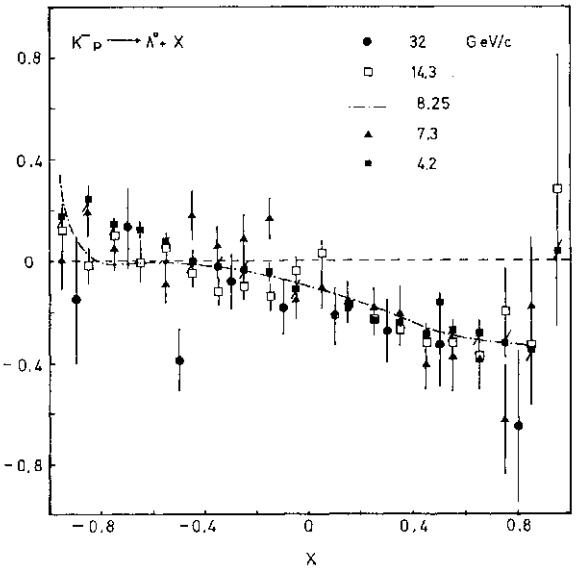

Fig. 12. Compilation of ^-polarization for K~p-* *A°+X* at 4.2, 7.3, 8.25, 14.3 and 32 GeV/c.[14]

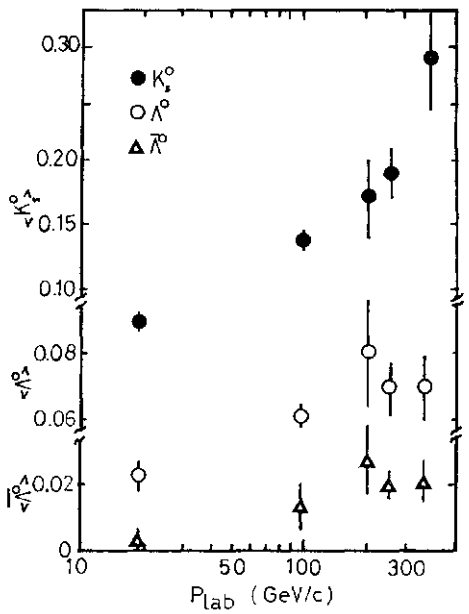

Fig. 13. Average number of K_{s}°, A^{o}, and A^{o} per inelastic collision, as a function of lab momentum.[15]

y=0, as the. charged pion distributions. The *A°* and A^{o} are instead produced backward. The same features are also evident in the *F(x)* distributions of Fig. 15. As in the previous reactions, 3.4, the A^{o} distributions are explained assuming that the reaction proceeds *via* K and K* exchange.

3.6. K-p-+S~-\-X

The data for the *F(x)* distributions presented for this reaction at various energies indicate a slightly forward production of the *S~* (Fig. 1(YL **Thp** rpar.fi **nn merFmnisTn** siPprrK **to** hp

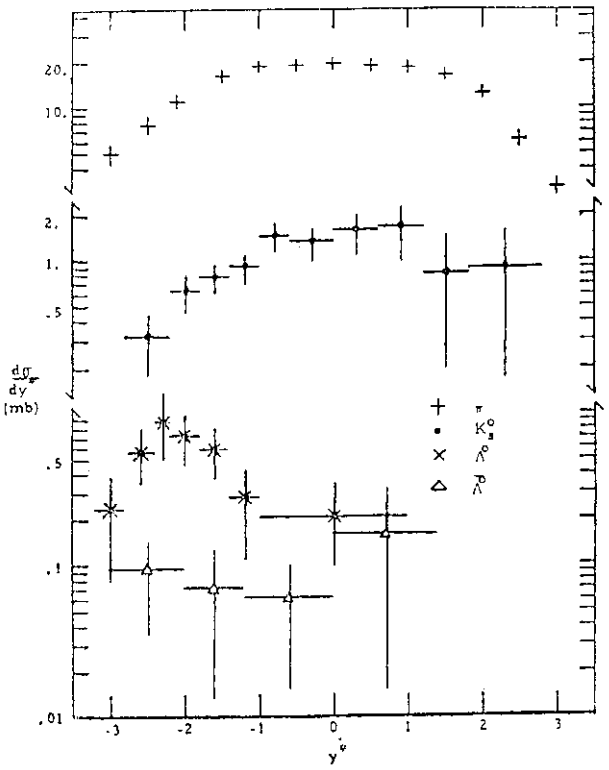

Fig. 14. Differential cross section *da/dy* as a function of cm. rapidity *y* for the production of K_s^0, A^0 and $\bar{A}^0$ in collisions at 360 GeV/c.[15]

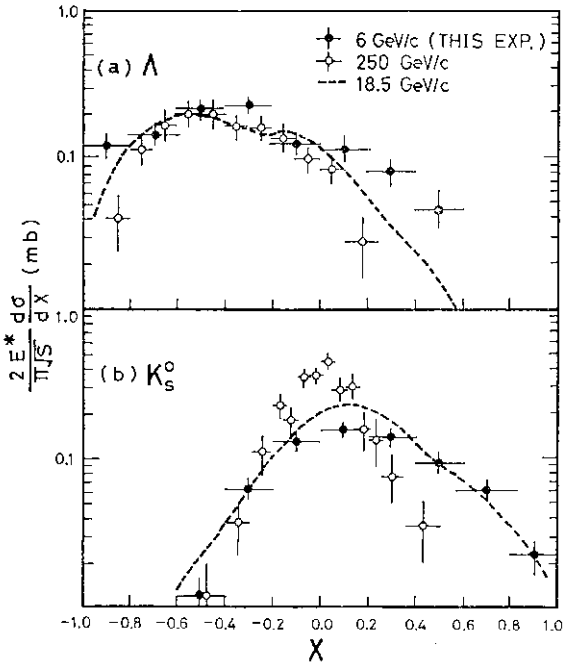

Fig. 15. x-distribution for A^0 and K_s^0 production in ::-p collisions at 6, 18.5 and 250 GeV/c.[16]

baryon exchange: a triple Regge formalism has also been used to interpred the forward production of E^-.[17]

§4. Survey Experiments

4.1. Hyper on beam

Figure 17 shows the results of a pressure

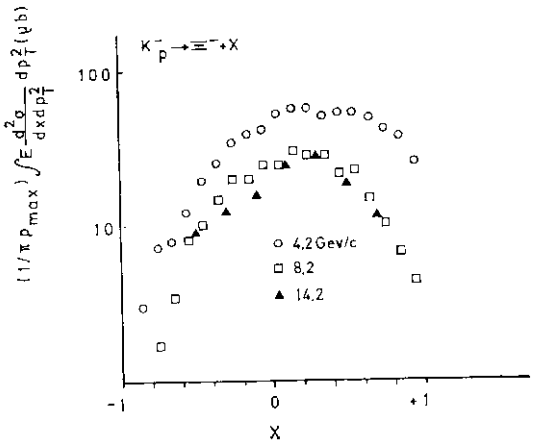

Fig. 16. Invariant cross section for the production of Ξ^- as a function of x at 4.2, 8.2 and 14.2 GeV/c.[17]

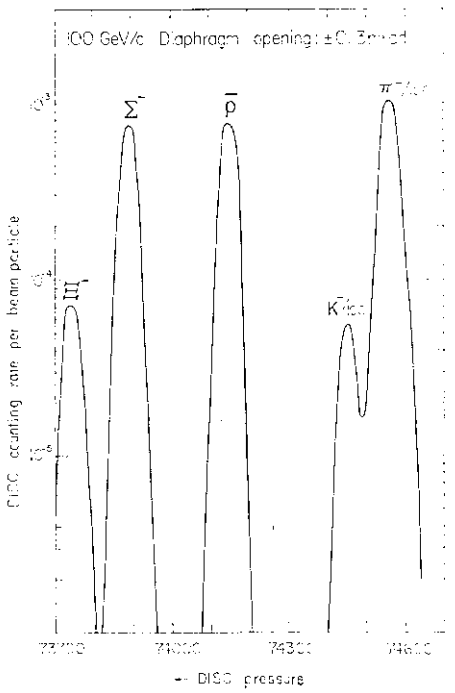

Fig. 17. Pressure curve with one differential Cerenkov counter in the CERN hyperon beam.[18]

curve obtained with one differential Cerenkov counter in the CERN hyperon beam[18]; Ξ^- and Σ^- are observed directly. The T^-, S^- and Q^- are instead seen only after reconstruction of their decays.

The CERN hyperon beam has typical fluxes of 400 S^- and 0.1 Q^- per pulse.

The measured particle ratios, Σ^-/π^-, S^-/Σ^-, have been fitted to a formula $(1-x)^{an}$ with reasonable fits. The $\bar{p}/\pi^-$, $\bar{\Xi}^+/\Xi^-$, $\bar{S}^+/S^-$ and $\bar{Q}^+/Q^-$ ratios decrease regularly, indicating a dependence on the strangeness of the baryon.[18]

4.2. Production of antinuclei

A compilation of the d/rr ratio measured at small p_t (<0.2 GeV/c) and low $x(x<Q2)$

plotted versus $p_{l\&h}$ shows that it has a strong energy dependence below 100 GeV/c, while above 100 *GeV/c* the dependence becomes less pronounced.[19]

The d production seems to take place in elementary pN collisions, while for the d production there are nuclear effects. In fact antideuterons production in p-Be and p-Al collisions yields the same results; while there is a factor of 1.4 for d-production. Moreover, the d production cross section in the pp c. m. system is peaked at x = 0 and seems to be symmetric about *x=0.*

The rates of production of p, d, t, p, d and t relative to pions of the same sign are plotted in Fig. 18 versus mass. Both nuclei and antinuclei have an exponential behaviour with mass. The slope for nuclei (~8 GeV^{-1}) is smaller than for antinuclei (~9 GeV^{-1}).

The production of nuclei and antinuclei in high energy pN collisions has been explained by using two (contradictory) models. In the sticking model, liht nuclei (antinuclei) formation occurs through the re-interaction of nucleons (antinucleons) created in elementary pN collisions. The model predicts $(o^{\wedge}/a_{s})\sim$ **tfp**$/(j_{p})^{A}$ where *A* is the atomic number and (j_{p} should be taken at the same velocity of the nucleus *A.* These ratios are off by about a factor of 3. Alternatively, thermodynamic models, predict direct production of nuclei-antinuclei pairs. The production cross sections should have an exponential behaviour in mass, with a slope $(2/r_{0})\sim 12.5\ GeV^{-1}$, where $T_{Q}\sim$ 160 MeV is the limiting temperature. The measured slopes are somewhat smaller than this value.

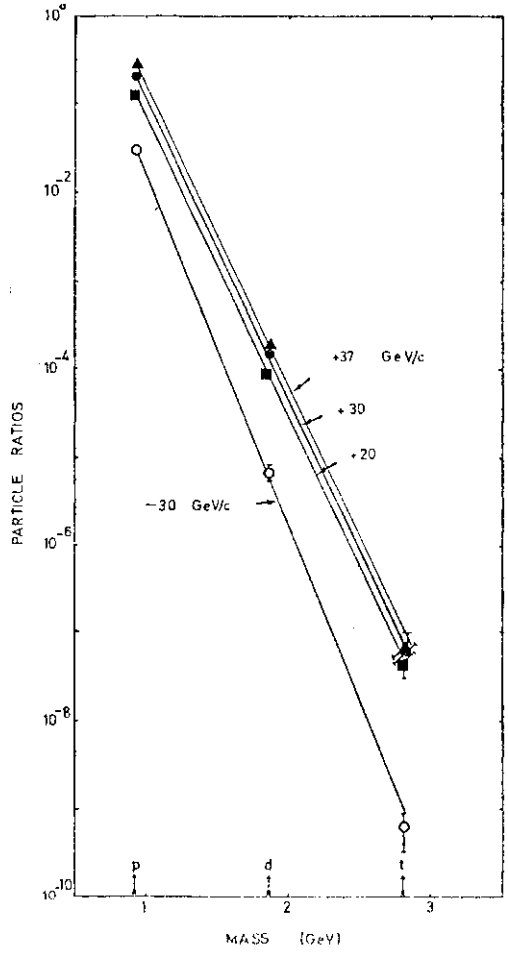

Fig. 18. Yields in the lab system of nuclei and antinuclei relative to pions of the same sign plotted *vs* mass.[19]

43. Limits on new particles

Four groups reported searches for new charged long lived particles in a secondary beam. These particles should have been produced in inclusive p-Be, p-Al collisions at 400 GeV at Fermilab, 200-210 GeV at CERN. The mass should have been determined from measurements of momentum-velocity, where the velocity was determined either with differential Cerenkov counters and/or time of flight. The electric charge was determined by pulse height.

The Fermilab experiments[20,21] were optimized for the search of particles with 5 GeV mass and unit charge. One of the CERN experiments[18] used the hyperon beam and was optimized for the search of large masses of short lifetimes; the other CERN experiment[22]

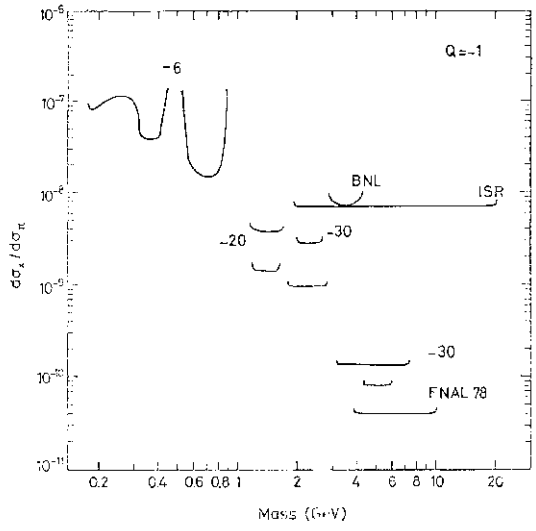

Fig. 19. Upper limits at the 95% confidence level for the ratio dtfjdov plotted *vs* mass m_{x} for particles with charge —I.[22]

	Cutts *et al.*[20]	Yidal *et al.*[21]	Bourquin *et al.*[1]*	Bozzoli *et al.*[22]
	FNAL	~ FNAL	CERN-SPS	CERN-SPS
p_0 (GeV/c)	400	400	200-210	200-210
p (GeV/c)	-70	-70	±95	±6, ±20, ±30, ±40
orange (GeV)	4-10	4.5-6	2-10	0.2-8
d(7/d^(95%C.L.)	4X10-[11]	lO"[10]	10"[7]	lO^-lO"[10]
G	-1	-1	±1	±2/3, ±1, ±4/3, ±2

was optimized for lower masses. The following table summarizes the main features of each experiment:

No good event was observed. Figure 19 shows in a graphical form a compilation of the upper limits obtained for charge —1.

§5. Conclusions

Many experimental papers were presented on the subject of this talk. The experimental situation has improved considerably, though it is still fragmentary. Among the many models used to interpret the data, the quark-parton and the triple Regge models are the more extensively used.

I would like to acknowledge the cooperation of many collegues and the warm hospitality of our Japanese hosts.

References

1. J. Whitmore: (Inclusive resonances production), Minirapporteur talk at this Conference.
2. M. Barth *et al.:* (Topological cross sections and inclusive A^0, K° and A^{++} production in K^+p interactions at 70 GeV/c), Paper 338.
3. J. M. Lafaille *et al:* (General features of the K"p interactions at 70 GeV/c), Paper 670.
4. D. Brick *et al:* (Topological cross sections for K^+p interactions at 147 GeV/c), Paper 616.
5. P. Slattery: (Evidence fo the onset on semi-inclusive scaling in proton-proton collisions in the 50-300 GeV/c momentum range), Phys. Rev. Letters 29 (1972) 1624.
6. W. Thome *et al.:* (Charged particles multiplicity distributions in pp collisions at ISR energies), MPI-PAE/EXP El 63 (1977).
7. I. Y. Ajinenko *et al.:* (Neutral pion production in K^+p interactions at 32 GeV/c), Paper 223.
8. J. R. Johnson *et al.:* (Inclusive charged-hadron production in 100-400 GeV p-p collisions), Phys. Rev. D17 (1978) 1292.
9. H. Weisberg *et al.:* (^-dependence of proton fragmentation by hadrons. II incident laboratory momenta 30-250 GeV/c), Phys. Rev. D17 (1978) 2875 and Paper 751.
10. D. Cutts *et al.:* (High energy inclusive scattering at Fermilab), Paper 413.
11. A. V. Barnes *et al.*: (Inclusive $n°$ and r production from 100 GeV/c p collisions in the Triple Regge region), Paper 1065.
12. A. V. Barnes *et al:* (Inclusive T T ° and ^ production in the all neutral mode from 100 GeV/c 7r~p collisions), Caltech Preprint (1978).
13. M. Baubillier *et al: (*A^0, *1°* and Y* inclusive reactions in K~p interactions at 8.25 GeV/c), Paper 433.
14. M. L. Faccini-Turler *et al.: (A* and *A* polarization in *X^p-^A/A+X* reactions at 32 GeV/c), Paper 225.
15. Y. P. Kenney *et al:* (Inclusive production of **7T°,** $K_s°$, A^0 and A^0 in 360 GeV/c **7r**"p interactions), Paper 501.
16. R. Sugahara *et al.:* (Inclusive strange particle production in -"p reactions at 6 GeV/c), Paper 547.
17. M. Baubillier *et al.: (E~* inclusive production in K"p interactions at 8.25 GeV/c), Paper 432.
18. N. Bourquin *et al.:* (Particle and antiparticle production by 200 and 210 GeV protons in the CERN-SPS charged hyperon beam), Paper 777.
19. W. Bozzoli *et al.:* (Production of d, t, He^3, d, t and HF by 200 GeV protons), Paper 915.
20. D. Cutts *et al.:* (A search for long lived heavy particles), Paper 653.
21. R. Vidal *et al.:* (A search for new massive particles).
22. W. Bozzoli *et al.:* (Search for long lived heavy particles in pN collisions at 200 GeV/c).

PROC. 19th INT. CONF. HIGH ENERGY PHYSICS
TOKYO, 1978

A 3

Inclusive Resonance Production

J. WHITMORE

Department of Physics, Michigan State University, E. Lansing, Mich.

§1. Introduction

In this review, the current status of inclusive resonance production is summarized.[1] In §2, the problems associated with determining cross sections are discussed. The energy dependence of the inclusive cross sections is reviewed in §3 and the dependence on Feynman *x* and transverse momentum squared *(jPT)* is presented in §4. Comparisons with quark-parton ideas are made in §5 and the consequences of resonance decays for single particle production are discussed in §6.

§2. Inclusive Mass Spectra

Until recently there have been relatively little data on inclusive resonance production at high energies. This is partly the result of cross sections which are smaller than those for inclusive single particle production *(e.g., a(p°)* ~ 10 mb, (7(5*° 1530)~ 10 *fib).* Furthermore, the difficulties of separating resonance signals from background are made worse at high energy because of the combinatorial problems. In addition, many resonances *(OJ\ p*[+], K*°- • •) are difficult to study inclusively because their decays involve 7r°'s which are generally hard to detect.

Among the reasons for studying inclusive resonance production are (1) resonance decays account for a sizeable part of the inclusive single particle production; (2) having non-zero spin, one can study the polarization for information about the production mechanism (although this will not be discussed in this report); and (3) there are models which make predictions for ratios of pseudoscalar to vector meson production.

Table I shows the contributions submitted to this Conference on inclusive resonance production. The problems of determining cross sections are related both to statistics and to the parametrization of the background. For experiments with low statistics one can use a hand-drawn background curve. However, for high statistics results such as shown[2] in Fig. 1 one can (a) use a polynomial in mass (or a polynomial in an exponential) plus a Breit-Wigner shape; (b) use a background obtained from exotic mass combinations *(e.g.,* T^TT* for *a(p°)* determination); (c) use a particle

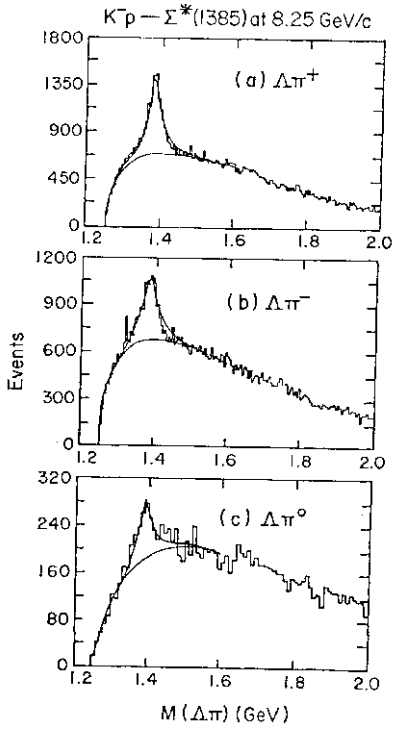

Fig. 1. Effective mass distributions from 8.25 GeV/*c* K~p interactions.
(a) *An*[+] (b) *An-* and (c) *An*[°].

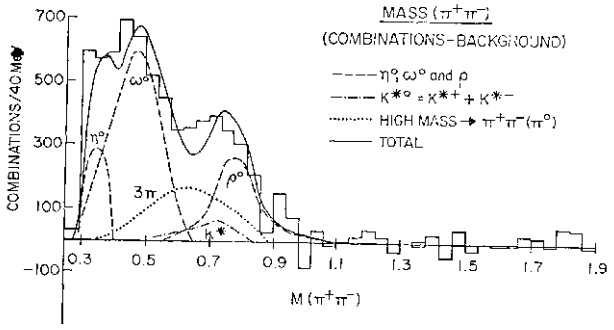

Fig. *2.* Correlated invariant mass from 300 GeV/c pp interactions obtained by subtracting the distribution found by associating *n*[+] and *n*~ mesons from different events from the observed *n*[+]*n*~ spectrum. The curves show the contributions obtained from various decays.

Table I.

Paper	Group	Reaction	(GeV/c)	Detector	Resonances studied
96l~~~	H. Saarikko "	7+p "	8~	81 cm HBC	,0° f°
690	IHSC	;:⁺p	147	30" HBC	J^{+} ⁺
547 ~~	KTOK	5 F p	6	KEK 1 m HBC	K*^ ^ "
208 «	JINR	***7z-p***	40	JINR 2 m Propane	/oV
1065	CIT-LBL	*rrp*	100	FNAL CTR	^+X°
			f 100		
499/500	NDF1MMTC	-"p	200	30" HBC	*r»* J^{+} ⁺
			{ 360		
690	IHSC	-~p	147	30" HBC	i⁺ ⁺
223	F-C-USSR	K⁻p	32	BEBC	***TJ***
338/1059	BCGMNST	K⁻p	70	BEBC	K*⁺
433	**BCGMF^**	K"p	8.25	2 m	*I*±
95	ABCLY	K-p	10,16	1.5 m, 2 m	a*⁰ (1530.
827	F-C-USSR	K"p	32	Mirabelle	J^{++} *Z*±
982	SRPG	K-p	70	BEBC	K*°
690	IHSC	pp	147	30"	+
495	T-S-K	pp	300	15'	^p°w° K*^ *Z*±
161	UCD-LBL	pp	400	15'	*y* ***CD°***
545/546/624	KOKO	pp	405	30"	*p°* f° K*^ *2*^
985	ARCHLMN	pp	1500	ISR	f° gK**°
862	B-C-P-M	pp	0.76	81 cm	K*⁺
549	T-T-M-F	pp	14.75	80 "	*2*±
610	A-D-H-M-P	pp	22.40	2 m Ludmila	J^{+} ⁺

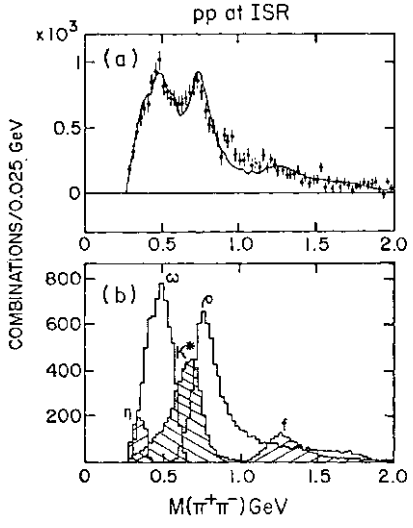

Fig. 3. >t⁻/t" spectrum from V *s* =*53* GeV pp interactions, (a) Best fit to the correlated *r^rr* spectrum with *p°, o),* K*, *f]* and f resonance terms (b) the individual contributions to part (a).

(E.G., K°, *TT")* from one event and combine it with 7r⁺⁻s from all the other events of the same topology, or (d) estimate cross sections by determining their contribution to reflections in other channels. This last method is illustrated in Figs. 2 and 3. In Fig. 2 the (7r⁻7r~) mass spectra after background subtraction (using method c) is fitted to a ***P°*** contribution, contributions from *7], o)° (via* their *TI⁺ TC~~* plus neutrals decay modes) and K*° *(via* its K^zr* decay with the misidentified as TT*), and a contribution from a high mass *TL^TZ'TT°* system. In this paper,[3] it has been assumed that <K*⁺ + K*-> = <K*⁰+K*°>~0.3. In another publication,[4] see Fig. 3, the K*° contribution was left free and no high mass *3?c* system included. The resulting <K*°+K*°> = 1.14±0.35is much larger than the directly observed (j(K*±) obtained in other high energy experiments. It remains to be seen whether this difference between *a(K⁺^⁻)* and 6r(K*°) is correct.

§3. Energy Dependence of Resonance Cross Sections

The cross sections for the most commonly measured resonances are shown in Figs. 4-7 as a function of the incident beam momentum.[5] In general one can conclude that at beam momenta above 100 GeV/c all of the inclusive meson resonance cross sections are increasing while the baryon resonance cross sections are falling or perhaps remaining constant. It should be noted that not all cross sections have been measured up to a few hundred GeV/c, and in fact some cross sections are

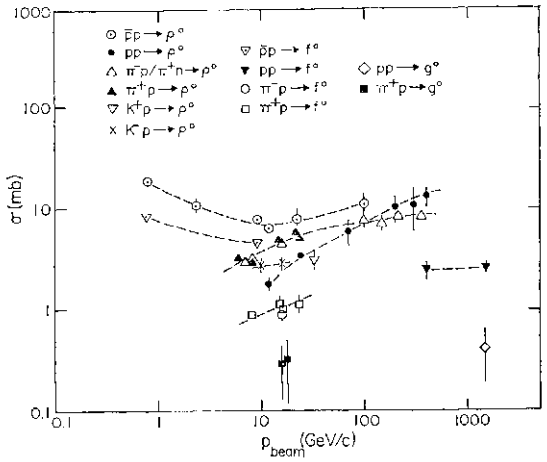

Fig. 4. Inclusive cross sections for $p°$, f° and g° production.

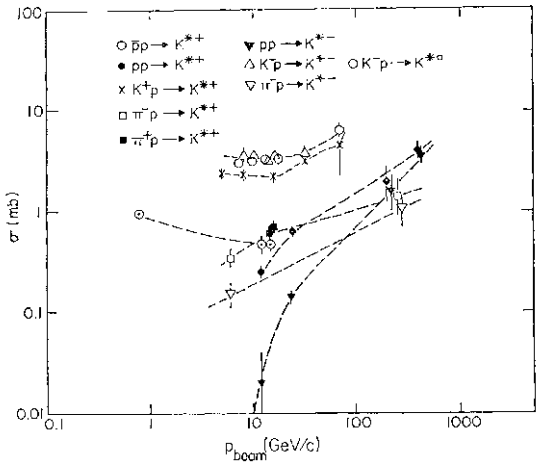

Fig. 5. Inclusive cross sections for K*±(890) and K*°(890) production.

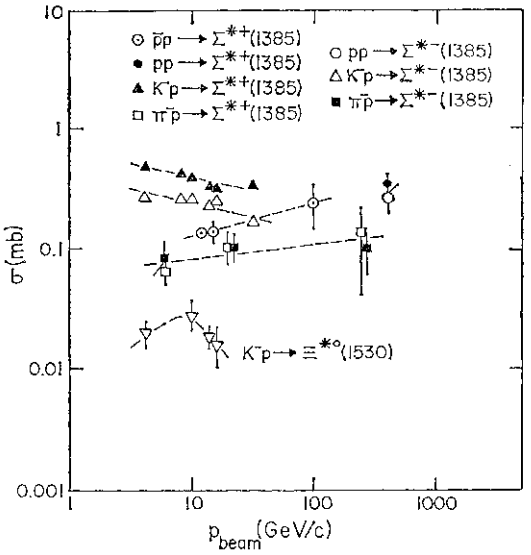

Fig. 6. Inclusive cross sections for 2·*±(1385) and £*°(1530)->£-7r⁺ production.

falling at the highest momentum that they have been measured *(e.g., o(f°)* in pp to ~9 **GeV**/c).

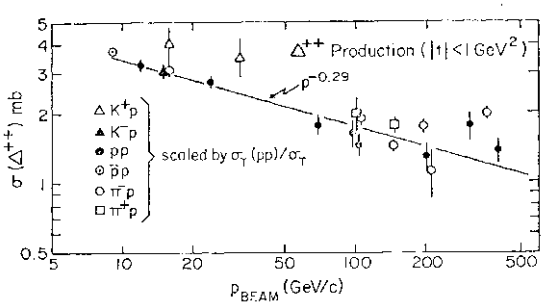

Fig. 7. Inclusive cross sections for $A^{*)}$ (1236) production.

Furthermore, the situation with regards the J^{++} inclusive cross sections is still unclear (Fig. 7).

§4. Dependence on x and p^

As examples of the *x* dependence of inclusive resonance production, Fig. 8 shows the *x* distributions for (a) pp^K*⁺ (890); (b) pp^ J*⁺(1385); and (c) K-p->£*°(1530)-+£-7r⁺. The K*⁺ is primarily produced in the central region,[6] *I*⁺ (1385) is produced primarily in the target fragmentation region,[6] and the *S*° (1530) is produced both in the central and beam fragmentation regions.[7] The *x* dependences for all reactions studied to any extent are shown in Table II. It is clear there is much work still to be done.

The*p*\ dependence (for K~p->2·*±(l 385) and K"p->£'*⁰(1530) for example) is shown in Fig. 9. One notes that all three resonances have a slope *B* (in $da/dp_T^2 = A \exp(-Bp_T)$ of about

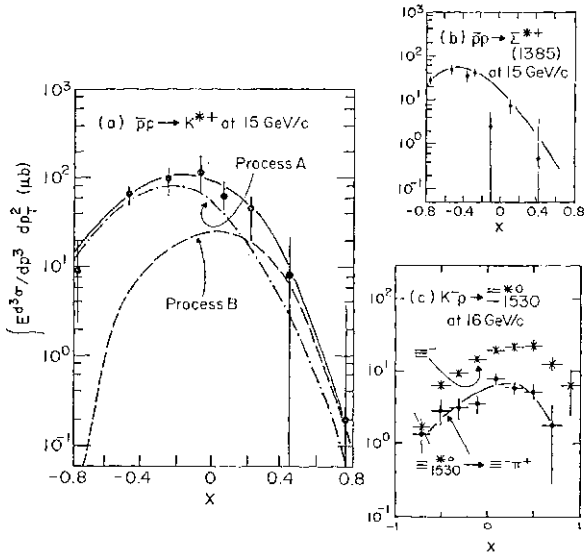

Fig. 8. Feynman *x* distributions for (a) pp->K*' (890) and (b) pp->J*' (1385) at 14.75 GeV/c. The curves are predictions from the quark model diagrams of Fig. 11. (c) K p >£*° at 16 GeV/c.

Table II. *x* dependence of cross sections. (T=target, C=central region, B=beam fragementation)

	7T⁻p	7T⁺p	K~p	K⁻p	pp	pp
1°	CB	CB				C
fo					C	
g°						
K*°			CB			
K* ⁺		CB		B	TC	TC
K*-					CB	C
K*(1400)						
j++	T	T	T	T	T	T
2'*⁺		T	TC		TC	TC
Z*-			C			C
£*°			C			

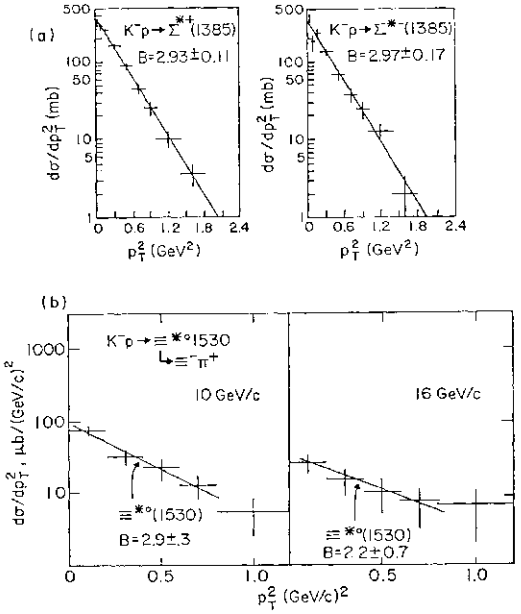

Fig. 9. *da/dpr²* for (a) K-p-*^** (1385) at 8.25 GeV/c and (b) K~p->£*° (1530) at 10 and 16 GeV/c. The solid lines represent fits to the form $da/dp_T^2 \sim A \exp(-Bp_T^2)$.

3 (GeV/c)"². Figure 10 (a, b, c) show that a value of $B \sim 3\text{-}4$ (GeV/c)⁻² is common to all processes studied. To summarize the $p\backslash$ dependences (a) $do\backslash dp\backslash = A \exp(-Bp\backslash)$ is a good representation of the data for $p\backslash > QA5$ (GeV/c)²; (b) inconstant for a given resonance at a fixed beam momentum, independent of incident beam particle; (c) *B* decreases slowly with increasing mass of the resonance,[8] (d) *B* decreases slowly with increasing beam momentum; and (e) *B* in pp annihilations is smaller than *B* in non-annihilation processes.[9]

§5.- Comparison with the Quark-Parton Model for Low jpT

In the most naive model one can discuss the

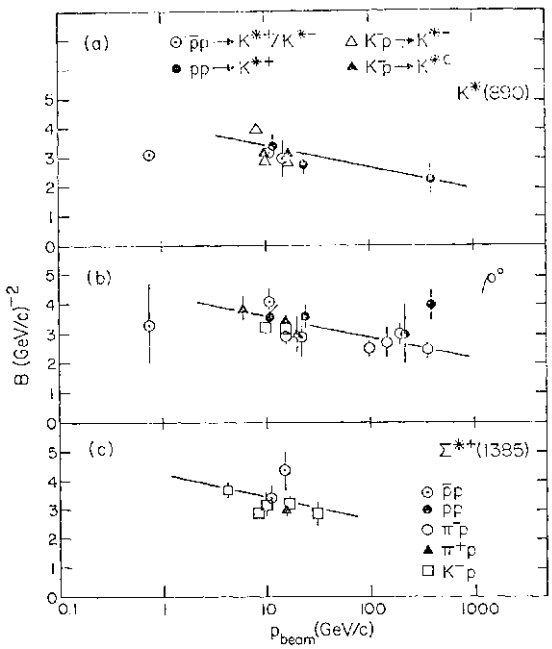

Fig. 10. Slope parameter, *B,* in $do/dp_T^2 = A \exp(-Bp_T^2)$ for (a) K* (890) (b) *p*° and (c) *I**+ (1385) production.

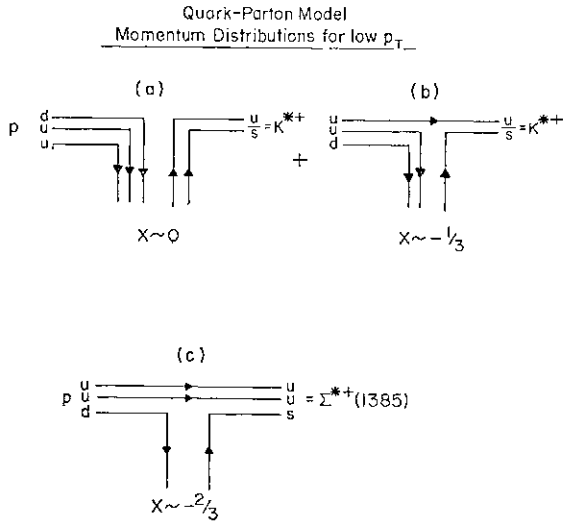

Fig. 11. Quark diagrams for pp->K*⁺ (890) and pp-^** (1385) production.

x dependence for resonance production in terms of the diagrams shown[6] as an example in Fig. 11. Figure 11(a) yields, assuming equal momentum partition among the three valence quarks in the proton, an *x* distribution for K*⁺ which is centered near *x=0.* Similarly Fig. 11(b) and (c) yield distributions peaked near *x*= —1/3 and *x*= —2/3 respectively. The results of using the quark momentum distributions obtained from a Drell-Yan analysis[10] of dilepton production are shown as the solid curves in Fig. 8. It should be noted that for the K*⁺(890) in Fig. 8(a) a ratio of 3.1 ±0.8 is found for the relative contributions

Table III. Comparison with quark-parton model for low p_T.

Reaction	Momentum (GeV/c)	Experiment	Theory (Ref. 11)
TT±P	16	^°=O.38±O.O6	0.14
		o>V=0.9±0.1	1
		f°/p°= 0.21 ±0.03	0.25
		<f>lp°<0.025	0.11
K-p	10-16	K*°//**o**°=2.36±0.30	2
pp	0.76 (Ann)	K*⁺/^°=0.054=b0.005	?
		K^+/KS$_{1r}$=0.79±0.09	3
	9.1 (Ann)	**o**/>°~l	1
	9.1 (Non-Ann)	fi>**V**=1.05±0.15	1
pp	12	**wV**=1.0±0.2	1
	24	*cD°/P°* = *1.0±0.2*	1
	400	K*⁺/i°°=0.3±0.1	0.33
		f°/p°=0.20 ±0.05	0.25
	1500	K**(1420)/f°=0.06±0.2	?

of Fig. 11(b) to 11(a). Excellent agreement between data and theory is obtained.

The quark-parton model of Anisovich and Shekhter[11] makes predictions for the ratios of various inclusive resonance cross sections. The comparison between experiment and the theoretical predictions is shown in Table III. Except for the *TJ/OJ ratio,* the agreement is rather good. It should be noted that the *co°/p°* ratio in 9.1 GeV/c pp annihilations has not been corrected for the indirect production of *p° via A^piz* decay. The authors state[9] that the agreement is better when estimates of this source of o°'s are taken into account.

§6. Effect of Resonance Decays on Single T T ^ K° and *A* Production

As we have seen, a considerable number of resonances are produced inclusively at high energies. It is important therefore to study the effects that these resonances have upon the inclusive single particle cross sections. Table IV shows estimates of the fractions of %~, *K* and *A* which are produced indirectly *via* resonance decay. In most cases equality of neutral and charged resonance cross sections has been assumed *[e.g., a(p°)^—a(p(p~)]*. We see that typically 45% of the TT~, 35-45% of the *Kl* and 17-30% of the *A* are produced *via* resonances. When one combines the various results and includes the effects of still higher mass baryon, hyperon and meson resonances it seems quite likely that only 10-30% of all pseudoscalar mesons are produced directly.

Table IV. Effect of resonance decays on % , K° and *A* production.

Reaction	Momentum (GeV/c)	*%rr* from Resonance	% K° from K*'s	*%A* from 2'*(1385)
7r-p	6		27±5	23.9±5
	16	46±4		
	20			25 ±10
	250		32±9	23 ±5
7T⁻p	15			23.4±5
	16	51±4	29±4	
K~p	8.25			25 ±5
	10		45±5	
	16		41 ±4	
	32			25 ±5
K⁻p	8.2		48±5	
	16		44±4	
	32		46±4	
pp	0.76 (Ann)	54±6	50±5	
	9.1 (Ann)	36±6		
	9.1 (Non-Ann)	60±6		
	12		23±4	25±4
	14.75		31±5	25±5
pp	405		52±10	30±4

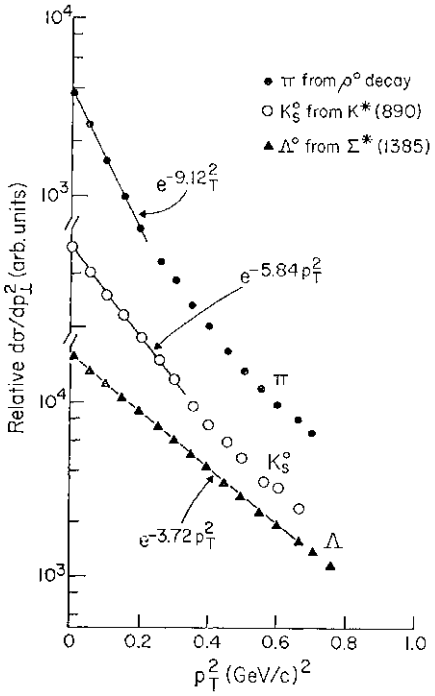

Fig. 12. p_T^2 distributions from Monte Carlo generated events for ***K*** (from *p°* decays), $K_s°$ (from K* (890) decays) and *A* (from **I'*** (1385) decays). The experimental *x* and p_T^2 distributions were used for generating K* and *Z** production. For *p* production, an exp $(-3.5p_T^2)$ dependence was used.

The effect of resonance decay on the single particle inclusive *p*\ distributions can be estimated *via* Monte Carlo calculations. As an example,[6] we show in Fig. 12 the Monte Carlo simulation of the 7r, *K*\ and *A* spectra obtained from *p*\ K*(890), and 2*(1385) production sith the known *x* and *p%* dependence for the resonance production. One notes that the *n* distribution has a slope $B = 9.12(\mathrm{GeV/c})^{-2}$, while the *K%* slope is 5.8 $(\mathrm{GeV/c})^{-2}$. Both values are significantly larger than those observed in Fig. 10 for resonance production. The slope for indirect *A* production is not very different from that for 2**0 385) production.

It is clear from the above discussions that the inclusive production of single particles at small |x| and *p%* is strongly effected by resonance production. In conclusion, there is still much work to be done in the study of inclusive resonance production since measuring the indirect *Kl* . . . production cross sections seems essential if we are to understand the inclusive single particle spectra at low *p%* and small *x*.

References

1. The discussion presented in the original talk on a comparison of multiparticle production with quark-parton ideas was based on papers submitted for publication in Phys. Rev. **D** (paper No. 267, 268) and is not reviewed here.
2. M. Baubillier *et al:* paper No. 433.
3. F. T. Dao *et al:* paper No. 495.
4. G. Jansco *et al:* Nucl. Phys. **B124** (1977) 1.
5. In addition to the papers shown in Table I, inclusive resonance cross sections are given in:
   (pp) V. Blobel *et al*: Phys. Letters **48B** (1974) 73; R. Singer *et al:* Phys. Letters **60B** (1976) 385; Nucl. Phys. **B135** (1978) 265.
   (pp) R. Hamatsu *et al:* Nucl. Phys. **B123** (1977) 189; C. K. Chen *et al*: Phys. Rev. **D17** (1978) 42; M. Markytan *et al*: Paper submitted to Strasbourg NN Conference (1978); D. Gall *et al:* Proc. Int. Symposium on NN Inter. (Loma Koli) p. 414 (1975); J. F. Baland *et al:* Nucl Phys. **B140** (1978) 220; R. Raja *et al:* Phys. Rev. **D16** (1977) 2733.
   (K^+p) P. Granet *et al:* Saclay preprint DPhPE 77-20 (1977); R. Barloutaud: Talk at Tbilisi Meeting (1976).
   (K"p) F. Barreiro *et al:* Nucl. Phys. **B126** (1977) 319; F. DiBianca *et al:* Phys. Letters **63B** (1976) 461; A. Vayaki *et al:* Nucl. Phys. **B58** (1873) 178; H. G. Kirk *et al:* Nucl. Phys. **B116** (1976) 99; H. Grassier *et al:* Nucl. Phys. **B118** (1977) 189; M. Bardadin-Otwinowska *et al:* Nucl. Phys. **B98** (1975) 418.
   (Λ^+p) H. A. Gordon *et al:* Phys. Rev. Letters **34** (1975) 284; M. Deutschmann *et al:* Nucl. Phys. **B103** (1976) 426; C. Baltay *et al:* Columbia Preprint (1978); H. Grassier *et al:* Nucl. Phys. **B132** (1978) 1.
   (~-p) J. Bartke *et al:* Nucl. Phys. **B107** (1976) 93; E. Balea *et al:* Nucl. Phys. **B54** (1973) 189; D. Fong *et al*: Phys. Letters **60B** (1975) 124; F. C. Winkelmann *et al:* Phys. Letters **56B** (1975) 101; D. Bogert *et al:* Florida State Preprint (1978).
6. J. Canter *et al*: paper No. 549.
7. ABCLV Collaboration: paper No. 95.
8. A similar effect has been noted in non-resonant systems, P. Stix *et al:* Phys. Rev. **D16** (1977) 558.
9. M. Markytan *et al:* ref. 5.
10. F. T. Dao *et al:* Phys. Rev. Letters **39** (1977) 1388.
11. V. V. Anisovich and V. M. Shekhter: Nucl. Phys. **B55** (1973) 455.

PROC. 19th INT. CONF. HIGH ENERGY PHYSICS
TOKYO, 1978

A 3 Rapidity and Charge Correlations

V. P. KENNEY

Notre Dame-Duke-Iowa State-Maryland-Michigan State-Toronto-McGill-Fermilab Collaboration

§1. Two-Particle Correlations: Energy and Multiplicity Dependence

Central-region hadrons produced in high energy inclusive reactions are emitted in "clusters," correlated in rapidity. It seem unlikely that conventional resonance can account for most of the correlation observed, except at low multiplicities where diffraction dissociation is important. With the usual definitions:

$$pi(y)=a \qquad 'da/dy,$$

the single particle rapidity density;

$$P2(yi,y2)=<r \qquad {}^{x}d^{2}ojdy_{i}dy_{2},$$

the two particle density; we study

$$Rn(yi,y2)=Rn(dy, \qquad y+)$$

$$=[(i02O>i, \qquad yJ/piiyMytJl—l,$$

the normalized semi-inclusive correlation function, for each multiplicity at four energies for 7T~p collisions at 18.5, 100, 200 and 360 GeV/c.

Semi-inclusive correlations at 360 GeV/c are shown for $n=4$—20 in Fig. 1. For unlike (—[-) pairs, Fig. la, significant correlation near $\wedge = 0$ is evident for all orders of charge multiplicity n. Values of $R_{n}(0, 0)$ for 360 GeV/c data are shown in Fig. 2a; $R_{n}(0, 0)$ as a function of s for $n=\%$ multiplicity (for $n<(n)$, diffraction dissociation is not negligible)[1] is shown in Fig. 2b. The data of Fig. 2 may be fit with a cluster model incorporating a narrow cluster multiplicity distribution[2] for which Berger shows

$$R\,i\,o\,o\,r- \qquad {}^{L\,N\,V} \qquad <*>\bullet'....\bullet \qquad <*> \qquad {}^{:}\ "I \qquad (1)$$

Fitting the two distributions jointly yields the measurement of cluster parameters: cluster

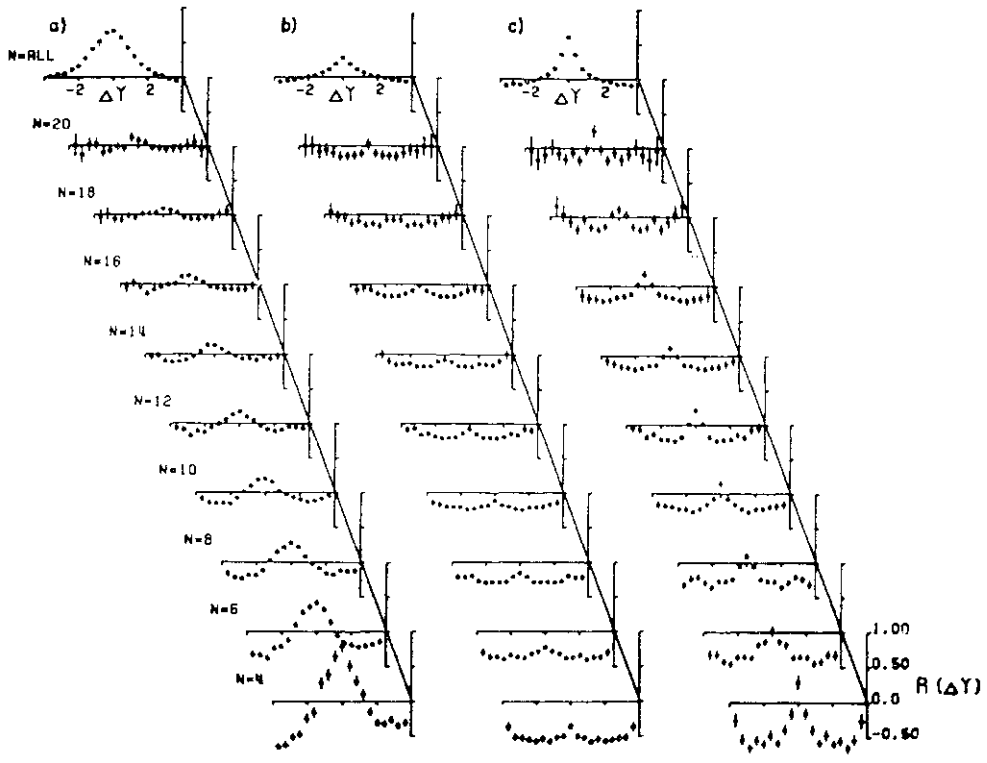

Fig. 1. Semi-inclusive correlations $R_{n}(dy, y)$ as a function of Ay, integrated over a central region —4.05<^+<4.05, for the data at 360 GeV/r. (a) Correlations for (— - **f**) pairs, (b) Correlations for (——) pairs, (c) Correlations for (——) pairs for which the azimuthal restriction ^<45° is imposed.

multiplicity $\langle k \rangle_{\sim^{+}} = 1.60 \pm 0.12$, correlation length $<3 = 0.99 \pm 0.03$. The data are inconsistent with Berger's expression for a broad multiplicity distribution.

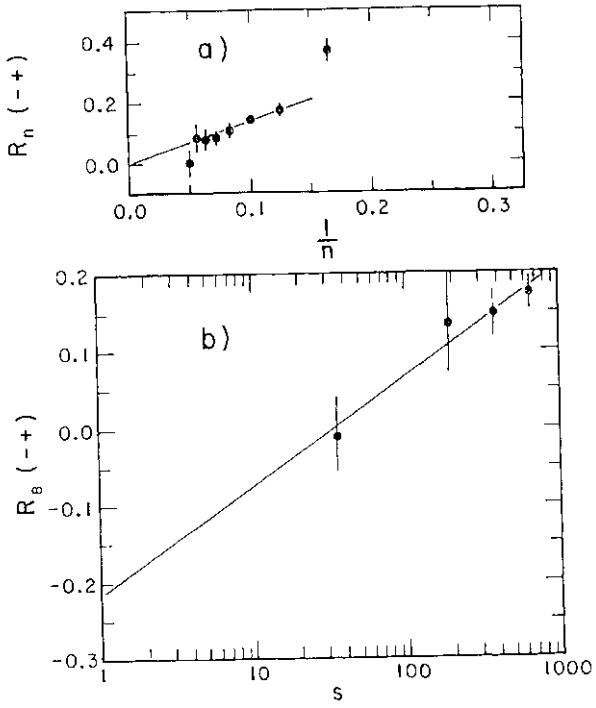

Fig. 2. Energy and multiplicity dependence of the correlation functions for (— - **f)** unlike-charge pairs, (a) $R_n(0, 0y^{+}$ as a function of *l/n* for 360 GeV/c interactions, (b) $R_n(0, 0)_{\sim^{+}}$ as a function of *s* for w=8 events.

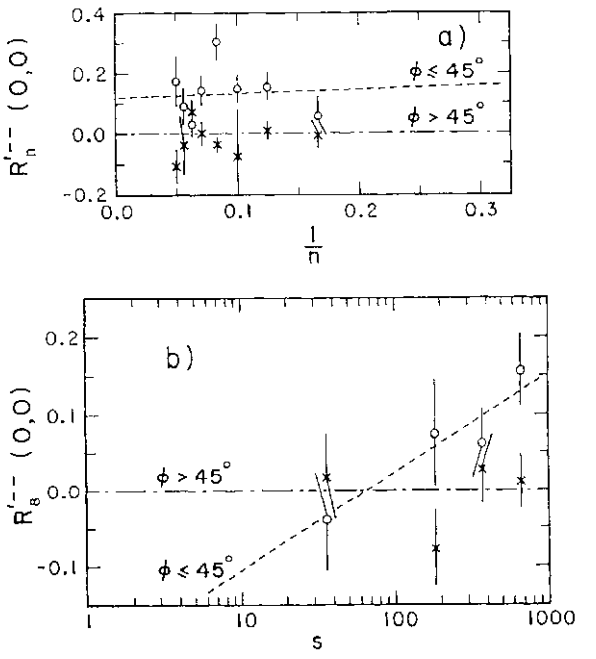

Fig. 3. Energy and multiplicity dependence of the correlation functions for (—) like-charge pairs, (a) **JV(0,** 0)-- as a function of *l/n* for 360 GeV/c interactions. Events for which $0<p<45°$. (Bose-Einstein cut) are shown as circles, $45° < \$5 < 180°$ as crosses, (b) $R_n'(0,$ 0) as a function of *s* for *n = S* events, with ^ cut as above.

For particle pairs of like charge, we attempt to distinguish the consequence of Bose-Einstein effects by distinguishing between all (——) pairs, Fig. lb, and (——) pairs for which which the azimuthal difference $0<45°$, Fig. la For like-charge pairs, the function $R'_n(y_i y^{\wedge}) = R_n + (l/n\_)$ is zero in the absence of correlation. This quantity is shown as a function of *l/n* for 360 GeV/c (——) data, and as a function of *s* for *n=8* data, in Fig. 3a and 3b respectively. Data for $0<45°$ (Bose-Einstein region) and $0<45^{o}$ are plotted separately. The correlation function for $ch<45°$ is consistent with zero for all orders of multiplicity, at all energies. We conclude that clusters are objects with small multiplicity <(£>, confined to a narrow rapidity range *8,* decaying predominantly to **(—h)** pairs.

§2. Three-Particle Correlations

If the conclusion above is correct, we would expect the 3-particle correlation to be a small effect. Previous experiments[3] have observed no clear evidence for 3-particle correlations^ within the limits of statistics. Taking $ps(y) = a_{\sim^{l}} d^{3}a/dy_1 dy_2 dy_3$, the normalized 3-particle correlation function

$$-R3O1,\ y^{*}>\ y^{\wedge} = |p^{\wedge} i y^{\wedge} \qquad y^{*}>$$
$$+2p_1(y_1)p_1(y_2)p_1(y_B) — p_2(y_1 y_2) \qquad (2)$$
$$pM \qquad -p^{\wedge} y^{\wedge} pM$$
$$— p^{*}(y^{*}> \ yi)pi(\mathbf{y2})]/[pi(yi)pi(yi)pi(yz)l$$

The terms in this expression can be understood more clearly by considering

$$R'siyu\ {}_{J>2,\ \wedge,)} = \mathbf{I} > 3(\wedge i,\ y\%| >'s)$$
$$-pMpMpMVipiiydpMpMl$$

the excess of the normalized 3-particle density over the combinatorial product of single particle densities, and

$$R'Ayi,\ {}_{J2,\ j>8)} = [|\mathbf{0}_{,}6>i,\ \mathbf{y2})pM$$
$$+/>2(j_{,,}\ y?)pi\{yi)+\mathbf{p2}\{y^{\wedge}\ j>iVi0>_{,})$$
$$+\ 3^{\wedge}\mathbf{I}(7|V|(72),0,(7,)]/[/>\mathbf{I}(7\mathbf{I}),\mathbf{OI}(72)^{\wedge}\mathbf{I}(^{\wedge}3)]. \qquad (3)$$

a background term arising from the presence of real 2-particle correlations in the data. Then the true, physically significant correlation

$$R^{*}(yu\ J2,\ yz) = Rz(y\pm,\ y\%,\ y^{\wedge} — Ri'iyu\ y^{*}>\ Js).$$

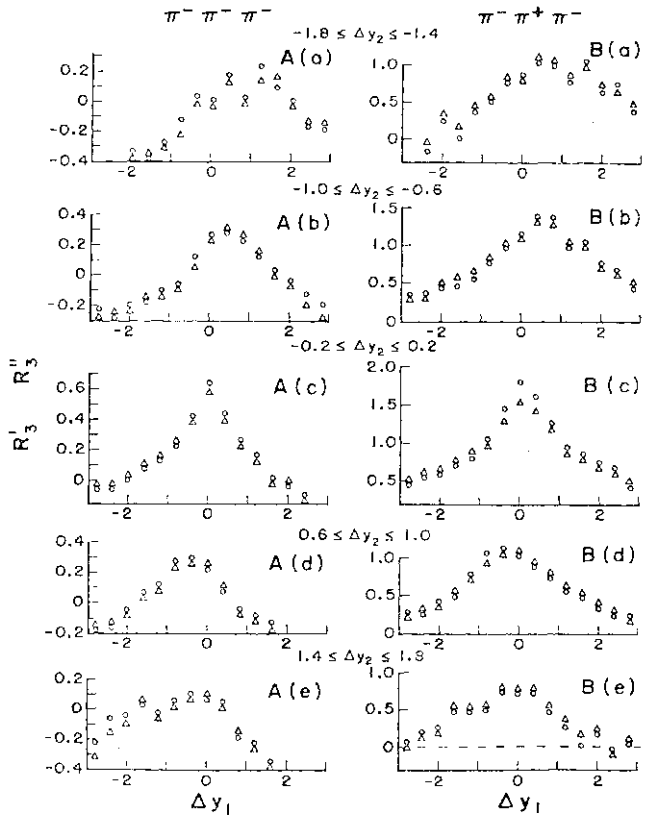

Fig. 4. Values of $R/(Ay_{19}\ Ay_{2})$ (circles) and $R^{\wedge}idy^{\wedge}\ Ay2)$ (triangles) as a function of $Ay_{1}=y_{1}—y_{2}$ for different intervals for $Ay_{2}=y_{2}—y_{x}$. Values for the (———) charge combination are shown on the left, A(a)-(e); values for the (—|—) charge combination are shown on the right, B(a)-(e).

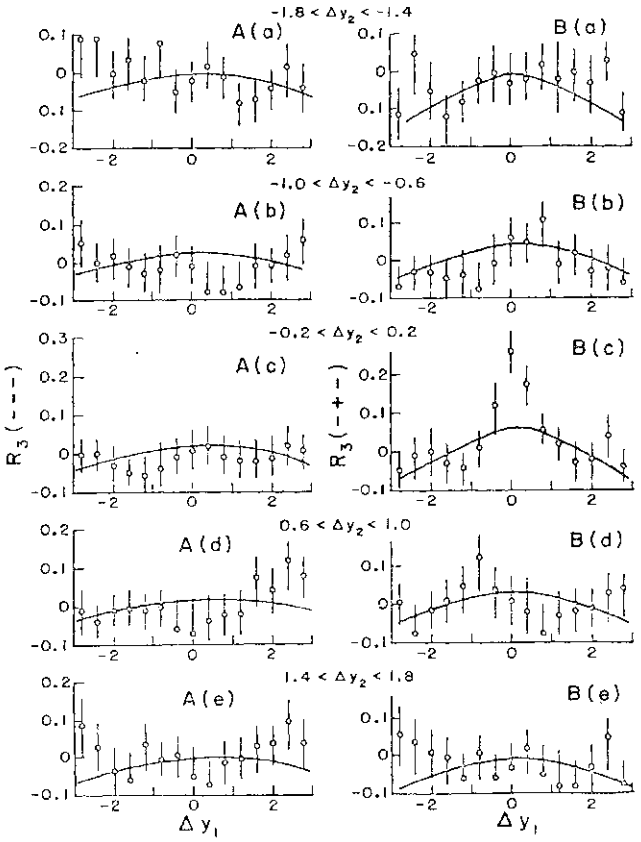

Fig. 5. Values of the true dynamical correlation $R_{8}(Jy_{19}\ \ Ay_{2}) = R/(Ay_{i},\ \ Ay_{2})\text{-}R/c\{Ay_{u}\ \ Ay_{2})$ as a function of Ay_{x} for various intervals of Ay_{2}. Values for the (———) charge combination are shown on the left, A(a)-(e); values for the (—+—) charge combination are shown on the right, B(a)-(e).

The signal R_{3} can be compared with the background term R_{3} for like-charge (————) and unlike-charged (—|—) 200 GeV/c data in Fig. 4. The only regions where a significant effect is seen is that in which $Ay_{x}=y_{x}—y_{\%}$ and $Ay_{2}=y2—ys$ are both small. The subtracted correlation i?$_{3}$ (— **1** —) shows a substantial peak in Fig. 5b(c), in contrast with the corresponding $R_{2>}$ (———) for like-charge data, Fig. 5a(c). It is clear that 3-particle correlations do exist; it is also clear that they are a small effect, consistent with the conclusions of the previous section.

References

1. F. T. Dao *et al* Phys. Letters **45B** (1973) 402; J. Lamsa *et ah:* Phys. Rev., to be published.
2. E. L. Berger: Nucl. Phys. **B85** (1975) 61 and private communication.
3. K. Eggert *et al:* Nucl. Phys. **B86** (1975) 201; M. Pratap *et al:* Nucl. Phys. **B116** (1976) 1; T. Kafka *et al.:* Phys. Rev. **D16** (1977) 1261.

PROC. 19th INT. CONF. HIGH ENERGY PHYSICS
TOKYO, 1978

A 3 Density. Charge and Transverse Momentum Correlations of Particles in Non-Diffractive p-p Collisions at V 5 =52.5 GeV

Presented by **H. D. WAHL**

CCHK Collaboration, CERN, Geneva

§1. Introduction

We present experimental results on particle as well as on charge and transverse momentum correlations in high multiplicity pp collisions at V *s =52.5* GeV/c and compare them with predictions of cluster models.

This study, performed at the CERN-ISR with the Split Field Magnet (SFM) detector[1,2] is based on 230 K events obtained with a "minimum bias" trigger, which required at least one reconstructable track in the detector. To minimize effects due to diffraction dissociation, only ~ 120 K events with an observed charged multiplicity larger than its average value were used.[1,3]

§2. Definition of Experimental Quantities

In addition to the smgle-particle and two-particle densities $p^{Q}(y)$, $p^{QQ'}(y, y')$ and correlation functions $C^{QQ'}(y, y')$ (Q, g'=sign of charge, y—rapidity) we use associated densities of particle number, charge and transverse momentum, defined as follows: The *associated particle density* $p^{QQ'}(y|y')$ is the density of particles of charge Q at rapidity y, conditional to the observation of a particle of charge Q' at rapidity y':

$$pW(y|y')=pW\{y,y')lp^{*}\{y') \quad (1)$$

Similarly, one defines the associated charge density $q(y|Q'_{9} y')$. To study charge compensation, we use the *associated charge density balance* defined by

$$My|y')=q(y|-,y')-q(y|+,y') \quad (2)$$

i.e., the change in the associated charge density at y when the particle of negative charge at y' is replaced by one with positive charge.

For the investigation of transverse momentum compensation, we use the associated compensating transerve momentum density:

$$\wedge T \wedge ')\,dy = -<S \wedge T i - (p i / | \wedge |)> \quad (3)$$

where the 2 is taken over all particles with rapidity y_i near y, and the average over all events with a particle near y'. Thus, $7i\wedge(y|y')$ is the total net component of transverse momentum (per unit of rapidity, at rapidity y) opposite to the direction of the transverse momentum p_T, of the particle at y'.

§3. Cluster Models[4]

The experimental distributions defined above are compared with predictions of different cluster models, which differ in their assumptions about the charge and transverse momentum dependence of cluster production:

Charge dependence:

IECC:[4] independent (random) emission of charged clusters (charge 0, ±1)

LCEX[5]: emission of charged (0, ±1) clusters with limited charge exchange (0, ±1)

IENC[6]: indpendent emission of neutral clusters.

Transverse momentum dependence:

UJM[7]: uncorrelated jet model

ULM[8]: uncorrelated link model (only correlations between adjacent clusters)

CLM[5]: correlated link model

Apart from the average cluster transverse momentum, all parameters of the model are determined from three experimental distributions (the correlation $C(y, 0)$ and the inclusive particle and charge densities $p(y)$ and $q(y)$). The values obtained are the following:

—mean charged multiplicity of cluster decay, $<£>\sim 1.8$,

—width in rapidity of cluster decay in its rest frame, $\wedge=0.67\wedge0.05$,

—density of clusters $p_c \sim l$ per unit of rapidity,

—average mass and charge of leading clusters $<M_L>=1.5$ GeV, $<£_L>>0.65$,

and all are in agreement with those obtained by other analyses.[4]

§4. Experimental Results and Comparison with Cluster Models

Charge correlation

The associated charge density balance $Jq(y_1|y_2)$ is shown in Fig. 1 as a function of y_x for 4 different values of y_2. The facts that the distributions are significanlly narrower than the corresponding particle densities, and that they have maxima at $y_x \sim y_2$ for all values of y_2, are a clear indication of local charge conservation. In Fig. 2, the charge density balance associated with a central particle ($|j_2|<1$) is compared with the cluster model predictions.

While both the IECC and LCEX models agree with the data, the IENC model predicts the charge compensation to be much more local than seen in the data and can therefore be ruled out. Since the IECC model predicts too high a long range component (See Fig. 6 of ref. 1), we conclude that the LCEX model is favoured by the data.

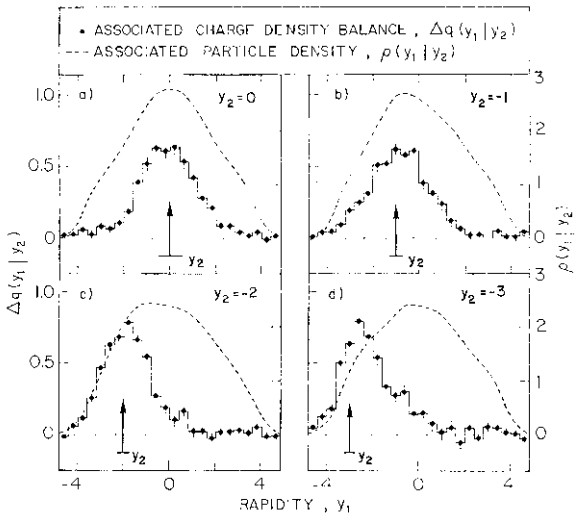

Fig. 1. Associated charge density balance $Aq(y_1|y_2)$ as a function of $y\pm$ for different values of y_2. For comparison, also the associated particle density $P(yi|y2)$ is shown (broken line).

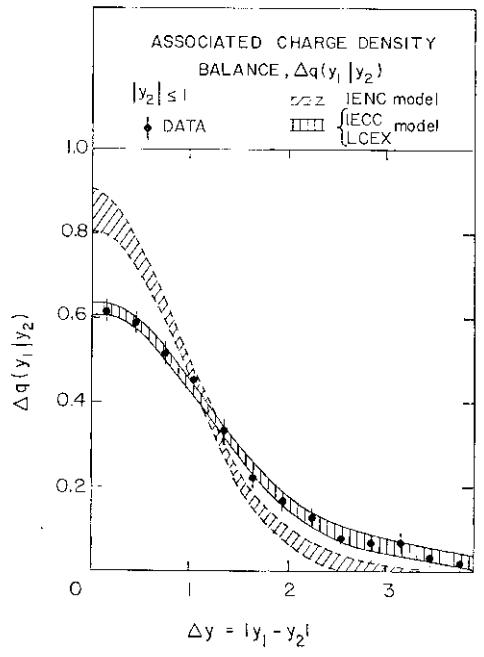

Fig. 2. Charge density balance $Jq(y_1|y_2)$ associated with a central particle flj^l^l) as a function of $dy=|yi—y_2|$* Also shown are the predictions of the IENC, IECC and LCEX models.

Transverse momentum compensation

The compensating transverse momentum density $x<j:(yi|y_2)$ (Fig. 3) shows a $y|$ dependence about as wide as the associated particle density; it does not change appreciably with y_2. This indicates that transverse momentum is conserved globally, or that the range in rapidity, over which p_T is compensated, is comparable to the total rapidity range available at our energy. A comparison of the average compensating transverse momentum density $nviyily*)$, defined by $7r_1(y_1|y_2)=7u_1(y_1|y_2)/p(yi|y_2)$, (see Fig. 4) with the cluster model predictions shows that the ULM model can be ruled out by the data. Both the CLM and UJM describe the data reasonably if one assumes that clusters are produced with an average transverse momentum $<(/\mathbf{r}_x>\sim 0.65$ GeV/c, and if a weight factor for the Bose-Einstein effect is included in the matrix element. Since in the framework of the UJM

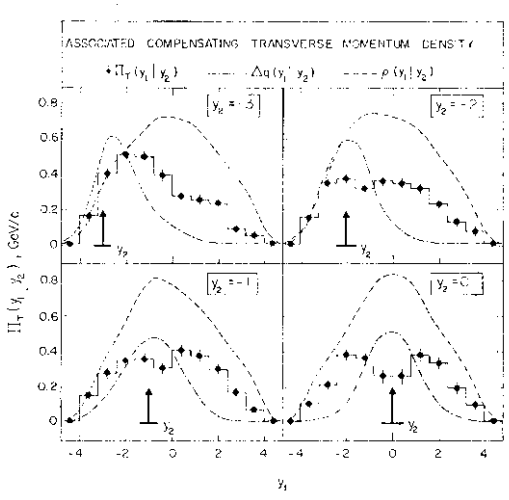

Fig. 3. Associated compensating transverse momentum density $7\boldsymbol{I}_1(y_1|y_2)$ *vs* y_1 for different values of y_2. For comparison, also the associated particle density $p(y_1|y_2)$ (dashed line) and charge density balance $dq(yi|y_2)$ (dashed-dotted line) are shown.

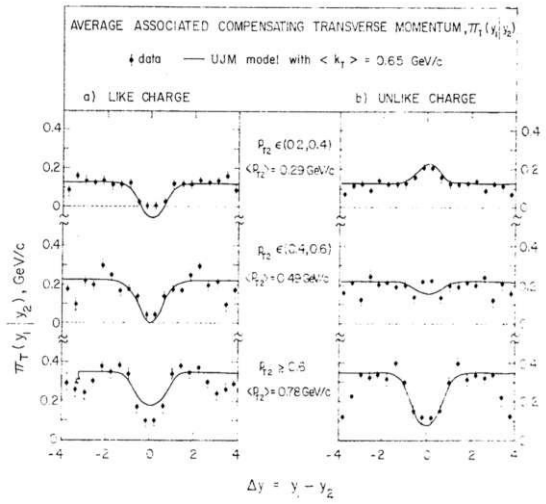

FIG. 4. AVERAGE COMPENSATING TRANSVERSE MOMENTUM $(\pi_T(y_1|y_2))$ *vs* $\Delta y = |y_1 - y_2|$, FOR $|y_2|<1$ FOR DIFFERENT VALUES OF p_{T2}; (A) FOR LIKE CHARGE PAIRS, (B) FOR UNLIKE CHARGE PAIRS. THE FULL LINE REPRESENTS THE PREDICTION OF THE UJM WITH $\langle k_T \rangle = 0.65$ GEV/C AND WITH A BOSE-EINSTEIN WEIGHT FACTOR INCLUDED IN THE MATRIX ELEMENT.

consistency between elastic scattering and multiparticle production requires small cluster transverse momenta, $\langle l \rangle \sim 0.1$ (GeV/c)[2],[9] we conclude that only the CLM provides a consistent description. In the framework of this model, the slope of the Pomeron trajectory is related to $\langle k_T \rangle$[10]; we obtain $a_p(0) \sim 0.26$ GeV~\ in good agreement with values found by other methods.[11]

§5. Conclusions

Charge is conserved locally in non-diffractive multiparticle production (rapidity range ~3)[5] while the range in rapidity over which transverse momentum is compensated is of the same order as the total rapidity range available. Particles of equal charge tend to be produced at small distances in phase space (Bose-Einsten effect). We find a radius i?= (1.34^ 0.31) fm and a lifetime =(1.38±0.60) fm of the pion source. A consistent description of the data is possible with a cluster model in which clusters are produced by a mechanism with limited charge exchange (LCEX) and with the transverse momentum dependence as given by the correlated link model (CLM with nearest neighbour links). The central clusters have an average mass of $\langle M_C \rangle \sim 1.3$ GeV, an average transverse momentum of $\langle k_T \rangle \sim 0.65$ GeV/c and decay on the average into $\langle k \rangle$= charged particles. Therefore, clusters seem to be very similar to meson resonances.

References

1. D. DRIJARD *et al*: PAPER 273.
2. M. DELIA NEGRA *et al:* NUCL. PHYS. B127 (1977) 1.
3. **W.** HOFMANN: REPORT KFK 2489 (1977).
4. A. ARNEODO *et al.:* NUCL. PHYS. B113 (1976) 156.
5. C. MICHAEL: NUCL. PHYS. B103 (1976) 296.
6. C QUIGG AND G. H. THOMAS: PHYS. REV. D7 (1973) 2752.
7. A. BASSETTO *et al.:* NUCL. PHYS. B34 (197]) 1.
8. J. L. MEUNIER *et al:* NUCL. PHYS. B87 (1975) 74.
9. F. HAYOT *et al.:* NUCL. PHYS. B80 (1974) 77.
10. M. LE BELLAC: CERN 76-14 (1976).
11. H.J. BEHREND *et al:* PHYS. LETTERS 56B (1975) 408.
12. D.S. *AyiQsetal:* PHYS. REV. D15 (1977) 3105.
13. H. J. BEHREND *et al:* DESY 78/26 (1978).

PROC. 19th INT. CONF. HIGH ENERGY PHYSICS
TOKYO, 1978

A3 Associated Multiplicities in Hadron Reactions

G. W. BRANDENBURG

MIT, Cambridge, Mass.

One of the simplest correlations that can be studied for multiparticle reactions is the associated charged multiplicity, n_x, which is defined as the charged multiplicity of the system X in the inclusive reaction $a+b \to c+X$. A somewhat naive interpretation to the variable n_x can be obtained from the following exchange diagram:

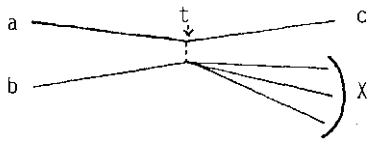

From this diagram we can interpret X as the final state of an interaction between particle b and a virtual particle of mass squared t. In fact this interpretation works remarkably well: n_x has the expected functional form $A+B \ln M$ over a wide range of M. As has been known for sometime, the constant B has the value 1.4 regardless of the identities of particles a, b and c, and is also equivalent to the coefficient of ln s in the expression for the total charged multiplicity. In a picture where high energy reactions have a rapidity plateau whose length is $\sim \ln sjM_aM_b$, B is just the linear density of charged particles along the rapidity chain. An additional feature of associated multiplicities is that they appear to obey the KNO scaling law initially proposed for the total multiplicity:

$$n_x P(n_x \mid n_y) = (n \mid n_y) \qquad (1)$$

There are several papers submitted to this conference which confirm the general features outlined above. For example, Fig. *1 shows the ln M dependence and the KNO scaling behavior of the $\pi^- p \to \pi^0 X$ data at 5 GeV/c submitted by a Dubna group.[1] Similar results were obtained by the ADHKMP collaboration[2] for the reaction pp->pX at 22.4 GeV/c.

Recent results from the Proportional Hybrid System Consortium[3] have shown that unlike B, the term A in the expression $A+B \ln M$ does depend on the particles involved, and

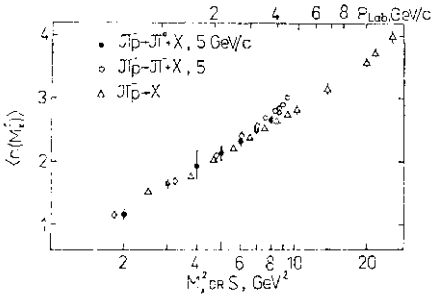

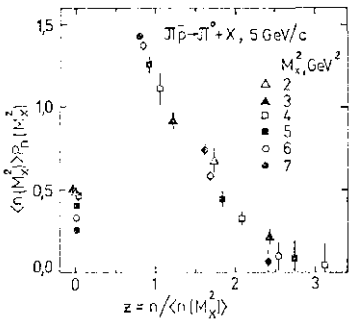

Fig. 1. (a) The average associative multiplicity vs M or s. (b) Plot of $n_x p_n(M)$ vs $z = n_x/n_i(M_x^2)$ for the reaction $\pi^- p \to \pi^0 X$ at 5 Gev/c.

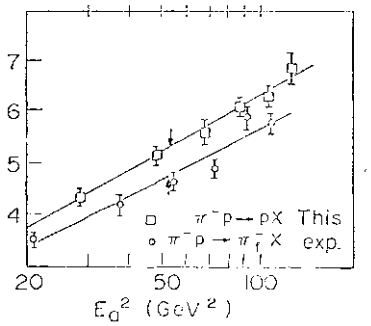

Fig. 2. Associated multiplicity for the reactions $\pi^- p \to pX$ and $\pi^- p \to \Lambda_{ast} x$ at 147 GeV/c as a function of the square of the available energy.

probably also on the value of /. This is shown in Fig. 2 where data on the reactions $\pi^- p \to \pi^- \pi^+_{ast} x$ and $\pi^- p \to p_{slow} x$ at 147 GeV/c are compared. Here n_x is plotted as a function of $El = Ml \sim M \setminus$ in an attempt to remove any threshold effects due to the mass of b.[4] Nonetheless there is an offset of about a half particle between the values of n_x for the reactions. This is interpreted as evidence that the pion

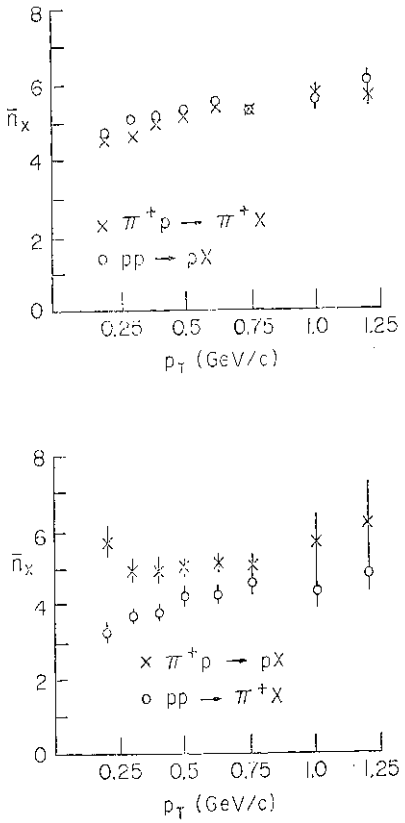

Fig. 3. Associated multiplicities as a function of p_T for the indicated reactions with p_{beam} = 100 Gev/c and x_i =0.6.

fragments into a larger number of particles than the proton does on the average. They propose that $A = n_b + n_{ac}$ where n_b is the average number of charged fragments from particle *b*, and n_{ac} is the same for the virtual exchanged particle coming from the *a—c* vertex. These fragments exist independently of the centrally produced particles whose average number is given by *B* In *M*\. In this notation their data show that $n_r > n_v$. A Weizmann-Strasbourg collaboration[5] has investigated *r^n* reactions in the same framework. They find that $nS > n_v > n_n$, and in addition that $n_{np} > n_{vv} > h_{zz}$. Perhaps it is not surprising that charged particles have a larger average number of charged fragments.

The PHSC group[3] has also observed a *t* dependence for n_x in the reaction ;:~p->7r~x Fitting their data for all values *M*\, they find that n_x increases linearly with *t* with a coefficient of (1.15±0.18). The reaction **7r**~p-> pX, however, has little, if any, dependence of n_x on *t*.

A Bari-Brown-CERN-Fermilab-MIT collaboration[6] has presented new data on associated multiplicities from a counter experiment at Fermilab. They have used the FNAL Single Arm Spectrometer to measure inclusive spectra at 100 and 175 GeV/c and have supplemented the spectrometer with a multiplicity detector surrounding the hydrogen target. The detector consists of a barrel shaped scintillation counter hodoscope, a set of proportional planes, and a forward hodoscope. Figure 3 shows preliminary data from this group on the reactions **(7r**$^+$,p)+p->(;r$^+$,p)+X at 100 GeV/c. The data for n_x is displayed as a function *ofp*$_T$ at x_F=*0.6.* This represents only a small fraction of the ~300 kinematic points measured in this high statistics experiment. Several observations can be made from the data shown here. First, n_x is identical for the channels **7**:$^-$p**->7r**$^+$X and pp->pX; this means $n^{\wedge} = n_{pp}$ which disagrees with the Weizmann-Strasbourg results. Secondly there is little variation of n_x with p_T for these channels, which is in disagreement with the *t* dependence found by the PHSC group (solid curve). The counter data do show an increase of n_x with p_T for lower values of x_F, however. Finally the dramatic difference between the 7r$^+$p->pX and pp->7r$^-$X data is probably the result of the requirement of a proton at large x_F in the pion induced reaction.

REFERENCES

1. N. S. Amaglobelli *et al:* paper No. 881.
2. A. A. Loktionov ***et a l :*** paper No. 213.
3. Proportional Hybrid System Consortium: Phys. Rev. Letters **37** (1976) 736; and paper submitted to Phys. Rev. **D.**
4. J. Whitmore and M. Derrick: Phys. Letters **50B** (1974) 238.
5. Y. Eisenberg *et al.*: paper No. 782.
6. D. Cutts ***et al.:*** paper No. 414.

PROC. 19th INT. CONF. HIGH ENERGY PHYSICS
TOKYO, 1978

A 3 Recent Results from 32 GeV/c K⁺p, K⁻p and pp Interactions

F. VERBEURE

Universitaire Instelling Antwerpen, B-2610 Wilrijk and
Inter-University Institute for High Energies, ULB-VUB, Brussels

§1. Introduction

I report on some results in K⁺p and pp interactions at 32GeV/c which have been submitted to the conference and not covered by Giacomelli.[1] All data were obtained in the 4.6 m MIRABELLE H_2 bubble chamber by the France-Soviet Union and CERN-Soviet Union Collaborations listed in ref. 2.

§2. Exclusive Reactions: Impact Parameter Analysis[6]

The reactions K⁺p->K⁺p7r⁺7r⁻ (reaction *A)* and K⁺p->K⁺p27r⁺27T⁻ (reaction *B)* were analyzed at 8.25, 16.0 and 32.1 GeV/c and the reaction **K⁺p->K⁺p** *3X+3TI-* (reaction C) at 32.1 GeV/c. We applied both the Webber method[3] and the Henyey-Pumplin (HP) method[4] to estimate the lower bound of the average impact parameter. The most important results are the following:

i) although the HP method systematically yields higher values of *(bl)* than Webber's method, the difference is not considerable;

ii) application of both methods is hazardous in those cases where phase space strongly affects the values of *(pn'Pii)* and leads to considerable overestimation of the bounds, *e.g.,* in the diffractive regions;

iii) if one constructs a simple amplitude, incorporating uncorrelated emission *at fixed rapidity* and leading particle effects, one can calculate the overlap function and the slope at /- 0 of the overlap function is a direct measure of (b^2). This method gives approximately the same values as the HP method;

iv) the energy dependence of (b_c) is shown in Fig. 1: an increase with energy, possibly to an asymptotic value is observed;

v) the (b_h) in the diffractive regions of reaction *A* are independent of the masses of the (K⁺7r⁺7r") and (p7r⁺7r⁻) systems.

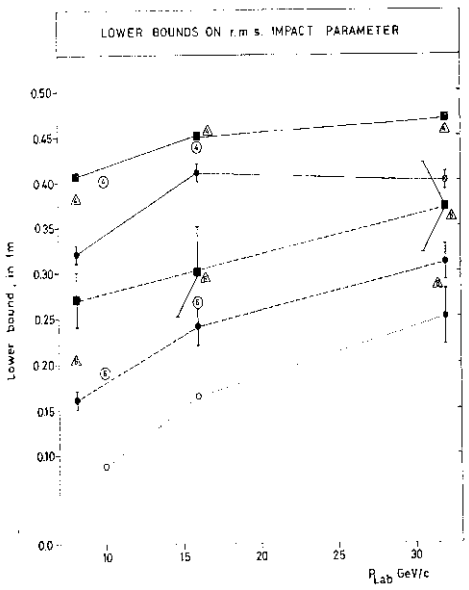

Fig. 1. Lower bounds on rms impact parameter for reactions (a)-(c) and comparison with corresponding K⁻p reactions.
• **(0)** Webber bound for K⁺p(K⁻p) reactions; figures in symbols indicate multiplicity of reaction.
• Overlap function bounds for K⁺p reactions.
A "lower bounds" equal to experimental value of

full lines: *K⁺v->K⁺px⁺x⁻*
dashed lines: K⁺p->K⁺p *2(n+n⁻)*
dotted lines: K⁺p->K⁺p 3(TT⁺^-)

§3. Semi-Inclusive Single Dissociation[6]

Kaon dissociation: the method used was based on a comparison of the missing mass distribution MM_p in the reaction K⁺p-» p+X to the missing mass distribution MM_A++ in the reaction K⁺p->J⁺⁺+X, where no Pomeron exchange is expected. Kaon diffraction is almost only observed in two-and-four-prong. 70 % of the diffraction cross section is found in the 4C channel K⁺p7r⁺7r⁻. On the 70 *pib* level there is no signal of kaon diffraction into 5 charged particles.

Proton diffraction: the method used is based on a comparison of laboratory momentum distributions of fast charged kaons and neutral kaons. Proton dissociation is found to be essentially constrained to 2 and 4 prongs, again more than half of the 4 prong dissociation

contains no single neutral particle. Factorization between K^+ and K~ induced reactions is found to hold within one standard deviation for 2 and for 4 prongs separately. The total inclusive single proton dissociation cross section is the same for K^+p and K~p interactions. In order to test factorization at different energies one may compare the ratios

$$\frac{i}{\text{o\{p~^p}_{0}\text{-^i charged particles)}} \qquad (1)$$

Figure 2 shows these ratios for z=1, 3 and 5. The ***7i~p*** data seem to be systematically higher but this may be due to the use of different methods. The data are too inaccurate to draw firm conclusions. Finally, examining the ratio i?t^{a}otai$^{o\,n\,e}$ observes a slight increase with enerev. nerham as In *s.*

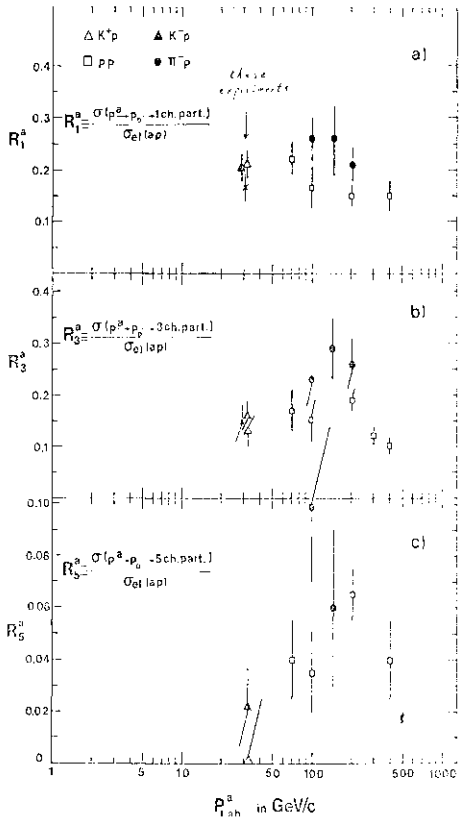

Fig. 2. Energy dependence of the ratio of topological diffractive (single vertex) proton dissociation to elastic scattering for various incoming particles.

§4. Inclusive Slow Proton Production[7]

A combined study was made of the reaction $K^+p \to p+X$ at 16 and 32 GeV/c with slow identified protons ($j?_{lab}$<1.2 GeV/c). The total cross section for the above reaction was found to be constant and equal to 5.94:0.1 mb which corresponds to 40% of the inelastic events. The da/dx distributions at fixed p_T are flat for x>—0.9 and energy-independent for ***pl>0A*** (GeV/c)^2. The structure function ***E-(Pa/dp****** however decreases systematically between 16 and 32 GeV/c for *x*>— 0.9 and (GeV/c)^2. Taken together, these two results imply that the proton carries away less energy at 32 GeV/c.

A simple triple-Regge fit with only one ***aiGLfltk*** term gives a fairly good parametrization in the interval $0.14<M^2/s<0.35$. The intercept a_t***(0)*** is close to one, except for $|f|<0.30$ (GeV/c)^2 and does not change when events of the subsample of $K^+p \to J^{++}+X$ events are removed. The trajectory *a^t)* however does change when removing these events.

About 40% of the $K^+p \to pX$ events have a K° in the final state, the cross section for $K^+p \to pK°X$ being (2.5±0.2) mb, of which ~0.3 mb can be attributed to beam diffraction dissociation.

§5. Inclusive 7r° Production[8]

In ^75% of the total available K^+p sample 17277 events were found with 19782 j-'s associated. The total cross section for $K^+p \to$;-X is 62±3 mb. From the M_{77} distribution (see Fig. 3) we estimate the TT' production cross section at $<7_{\mu}o=29\pm3$ mb and the *v* cross sec-

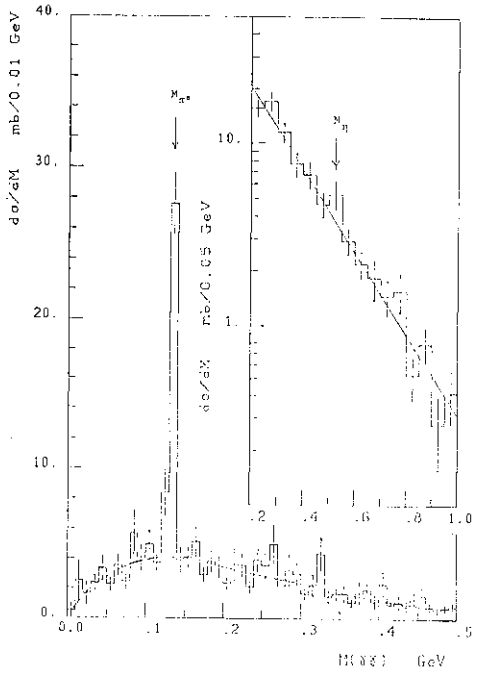

Fig. **3.** Effective mass spectrum of the **(77-)** combinations in 10 MeV intervals.

tion at $a_v = l.6 \pm l$ mb. The *S°(E°)* decay into *A°y(Aj)* was estimated at —0.2 mb. (~0.1 mb).

The *da/.dx* and *dajdp^* distributions of the 7r°'s could be obtained directly from reconstructed **7r°'s** as well as analytically from the]- spectrum, the two methods yielding compatible results. Comparing the distributions of the 7r°'s with TT"S one observes a stronger concentration around x=0 and at small *pi.*

§6. *A°* and *A°* Polarization in K⁺p Interaction[9]

The polarization was calculated for both the produced *A's* and i's in K~p as well as K⁺p interactions at 32GeV/c Giacomelli[1] has shown the K~p-»;f+X data at 32 GeV/c and a comparison with available lower energy data shows no striking energy dependence. Fig. 4 presents a comparison of the *A°* and the *A°* polarization in K⁺p interactions at 13 and 32 GeV/c. Within the large experimental errors, no change with energy is observed. The *A°* polarization in K⁺p and K~p interactions are to be fully compatible. A qualitative interpretation in terms of triple-Regge-exchange is attempted.

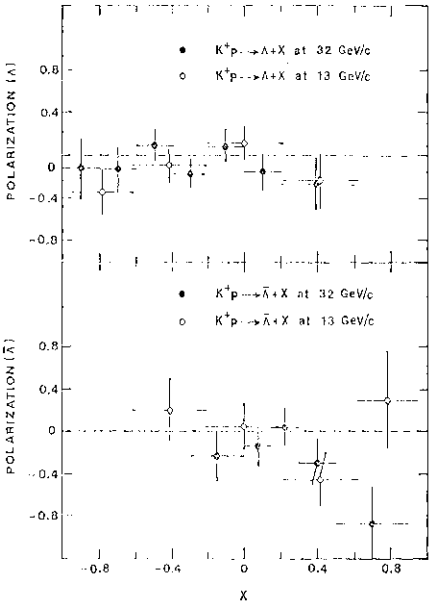

Fig. 4. Comparison of ***A*** and *A* polarization versus Feynman ***x*** in K⁺p interactions at 13 and 32 GeV/***c***.

§7. Analysis of Like-Particle Correlations[10]

Like-particle correlations can be parametrized as suggested by Kopylov, Podgoretsky and Cocconi[11]; in this framework they may yield information on the radius (R) and lifetime (r) of the emission volume and on the degree of incoherence (?) of the like boson field. A semi-inclusive study for $n^{ch}>6$ shows the following features:

i) *R* and r are independent of the charge multiplicity

ii) *1* decreases rapidly with increasing n_{ch}.

Acknowledgement

All credits of this work go the collaborations involved and all mistakes are to be blamed on the author.

REFERENCES

1. G. Giacomelli: Mini-rapporteur talk at this Conference, Session A3.
2. K⁺p: Brussels, Mons, Paris, Saclay, Serpukhov. K~p: Aachen; Berlin, CERN, Saclay, Serpukhov, Vienna, pp: Alma-Ata, Brussels, Mons, Moscow, Saclay, Serpukhov.
3. B.Webber: Phys. Letters 49B (1974) 474.
4. F. Henyey and J. Pumplin: Nucl. Phys. B117 (1976) 235.
5. E. De Wolf *et al*: paper 445.
6. J. Saudraix *et al.*: paper 224; A. Givernaud *et al:* paper 226; M. Jabiol *et al:* paper 228.
7. J. Laurent *et al:* paper 221.
8. I. V. Ajinenko *et al:* paper 223.
9. M. L. Faccini-Turleur *et al:* paper 225.
10. M. Goossens *et al*: paper 444.
11. For a review see M. Podgoretsky: Proc. Tbilisi Conf. 1976, A2-27.

PROC. 19th INT. CONF. HIGH ENERGY PHYSICS
TOKYO, 1978

A3 A Summary of the 400 *GeVIc* pp Data and Related Topics

Presented by **H. KICHIMI**

KEK

In this report we present data on resonance production in 400 GeV/c pp interactions and some comments on data in 6GeV/c 7r~p interactions.[1-4] The 400 GeV/c pp data come from the analysis of 50 K pictures of film taken at the Fermilab 30 inch bubble chamber, and the 6 GeV/c *x~p* data come from 200 K pictures from the first bubble chamber exposure made using the KEK lm bubble chamber.

A systematic study of single particle and resonance production is of great interest and importance in order to understand multi-hadron dynamics, since single particle spectra and particle ratios are strongly affected by resonances directly produced in the central and fragmentation regions.

From the phenomenological point of view, ratios of various mesons and scalar/vector/tensor ratios are among the most important information needed to probe several theoretical predictions based on the quark model. It should, however, be emphasized that there also exists a strong need for information on tensor mesons and baryon resonances.

Firstly, we present results on j£*(890), *K*** (1420), ^(770) and/(1270) meson production in 400 GeV/c pp interactions.[2,3] The effective mass distributions for (#>*) combinations show clear peaks of *K*⁺* and £*" in Fig. 1(a) and (b) respectively. A broad bump is also observed in the £** region, as shown in Fig. 1(c). This *K*** peak is more clearly seen if we plot the events with \x\ value between 0.1 and 0.2. The cross section values obtained are listed in Table I.

From the analysis of *x* and *p*\ distributions for *K*\ and *K** production, we have observed the following features.[2] Both *K*** are produced predominantly in the central region, |#|<0.2. In this region the ratio *K*⁺/K*~* is about one, whereas for |x|>0.2, it increases to about 3. A steeper slope of the *p?* distribution for *Kl* production is observed at

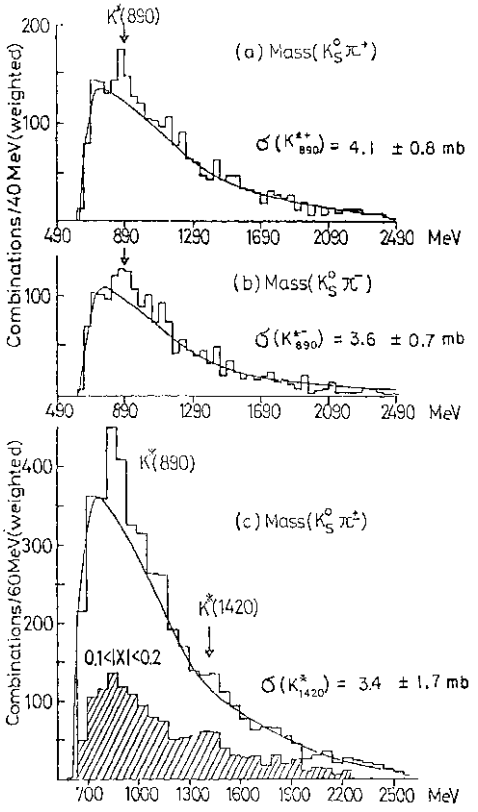

Fig. 1.

Table I. Cross sections for *p°*, *f*₀ Z*(890) and *K*** (1420) production.

(a) *P°QNTI* f

	cr mb	*I/P°* ratio	prediction
P°	13.5 ± 3.0		
		0.20 ± 0.09	^ 0.22
f J	2.5 ± 1.0*		

*cross section at P? greater than 0.6 (GeV/c)'

(b) K°, K*(890) K**(I420)

	cr .mb	*CR'* mb	ratios	prediction
Ks	7.43 ± 0.45	7,43 ±0.45	I	I
K*;	4.1 ±0.8"			
—^c + „ᵥ	3.85 ± 0.75	0.52±0.I0	0.53	-0.62
K 890	3.B ± *u.r*			
K"^T-				
		Q-	0.23±O.I2	O.I3 ~ 0.15

** combined cross section

(c) Direct production cross sections

	cr.. mb	cr. mb	
K	7.43 ±0.45	T 3 ~ ± 12	PS~
K..	3.85 ±0.75	3.4 ± 0.8	V
Kuzoi	I~7 ±0.8	[1.7~±" 0.8	_ _ _ _ [_

os *CRJ,=AJ* , cr,'ₛ.ₚ,27xcr,'+ crj

and C7,^cr,T.crv.crPs

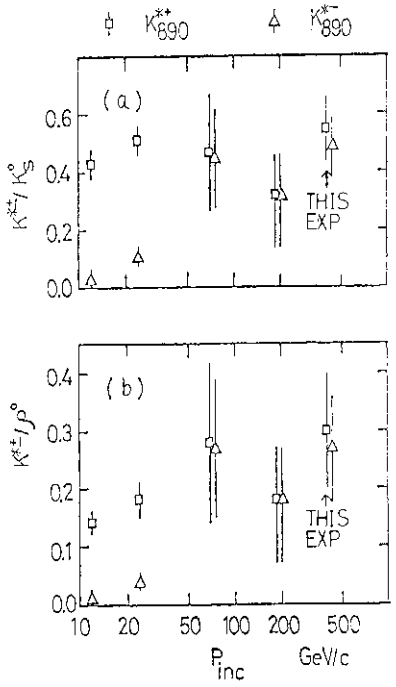

Fig. 2.

small />$_T$. This indicates a resonance decay effect.

Figure 2(a) shows vector/scalar ratios, together with data at lower energies.[2] The *K**~/Kl* ratio seems to be constant over the wide range of momentum between 12 and 400 GeV/c. Its value is obtained to be 0.55± 0.11. The *K**~/K°*$_s$ ratio is very small at 12 GeV/c, but increases with energy, becoming comparable with the *K**~/K°*$_s$ ratio in the hundred GeV/c region. Figure 2(b) shows *K^jp*^{0} ratios. The suppression factor for strange meson production seems to have a constant value (about 0.3) from 69 to 400 GeV/c.

In Fig. 3 we show the mass distribution of (7r~7r~) combinations with *PKx+x^KOti* (GeV/c)^2. The / meson peak is clearly seen.

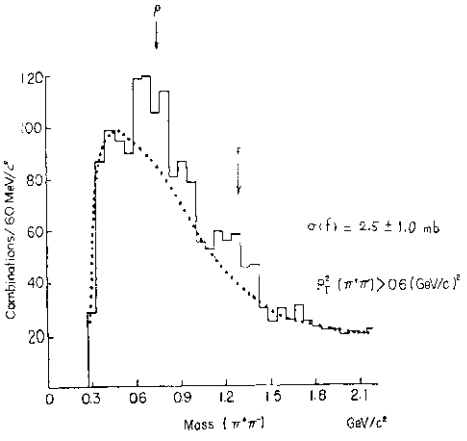

Fig. 3.

The cross section value is found to be 2.5±1.0 mb.

We have obtained vector/tensor meson production ratios for non-strange mesons in Table 1(a) and for strange meson in Table 1(b). The last column shows the predictions of the multiperipheral production model of Fukugita ***ET*** *al*[6] We obtain good agreement with the predicted values.

Table 1(c) shows the direct production cross sections for strange scalar and vector mesons. The value obtained for direct scalar *K* meson production is 2.3 mb. This indicates that less than one third of the scalar *K* mesons are produced directly. All these results may be understood in the quark model.

Next we present results on baryon resonance production, 2[7]*(1385) in 400GeV/c pp and 6 *GtV/c* ***7T***~*p* interactions.[1,4] We may expect some common behaviour in the proton fragmentation region even in these different interactions with a large difference of center of mass energy. We show a compilation of J* data in **7r**$^+$p and pp interactions (Table II).[7] An interesting result is the constancy of the *2**$^+$/A* ratio above 10 GeV/c, almost independent of beam particle. The constant value seems to be between 0.14 and 0.18.

Table II. 2^(1385) production cross section.

P_{inc}	beam	Λ	Σ^{*+}	Σ^{*-}	Σ^{*+}/Λ	Σ^{*-}/Λ
405	P	4.01 ±0.39	0.61 ± 0.13	0.45±0.11	0.15 ±0.03	0.11 ±0.03
24	P	1.76 ±0.06	0.28 ± 0.03	0.12 ±0.02	0.16 ±0.02	0.07±0.01
15	π^+	0.95 ±0.02	0.19 ± 0.04	0.03 ±0.01	0.20 ±0.04	0.033±0.012
15	π^-	1.27 ±0.05	0.17 ± 0.03	—	0.14 ±0.02	—
12	P	1.12 ±0.03	0.20 ± 0.02	0.07 ±0.01	0.18 ±0.02	0.06± 0.01
8	π^-	0.89 ±0.11	0.07 ± 0.02	0.09 ± 0.03	0.08 ±0.02	0.10 ± 0.03

A comparision of the *x* distributions for *A* and *2** in our pp and **7r**~p data shows a considerable increase in the *A* production cross section in the central region in our 400 GeV/c pp data. However, we observe a scaling of *A* production in the proton fragmentation region (|x|<0.6) even in the 6 GeV/*c* 7T~p data. We may also mention that the *2**~/A* ratio in 6 GeV/c *x'p* and 400 GeV/c pp data are very similar in the central region (|x|<0.2). The value of the ratio is found to be about 5.

References

1. H. Kichimi *et al*: Phys. Letters **72B** (1978) 411.
2. H. Kichimi *et al:* Contributed paper No. 545 to this Conference.
3. H. Kichimi *et al:* Contributed paper No. 546.
4. R. Sugahara *et al*: Contributed paper No. 547.
5. J. Whitmore: Phys. Reports **IOC** (1974) 273; **27C** (1976) 187.
6. M. Fukugita *et al*: Nucl. Phys. **B121** (1977) 93, and University of Tokyo preprint UT-281 (1977).
7. K.Bockmanne/tf/.: Report BONN-HE-77-21; C. Baltay *et al*: Columbia Univ. Preprint (1977). F. Barreiro *et al*: Phys. Rev. D17 (1978) 669;

PROC. 19th INT. CONF. HIGH ENERGY PHYSICS
TOKYO, 1978

A3 Some Features of pp Annihilations at Low Energies

H. YUTA

Bubble Chamber Physics Laboratory, Tohoku University, Sendai

For pp annihilations at low energies four papers have been submitted to this Conference: paper numbers 436, 862, 505 and 550. The first two papers have already been discussed in the previous talks. In the last two papers, preliminary results of the most recent data obtained from the ANL 12 foot bubble chamber with the track sensitive target (TST) were presented and will be reported in this talk. In particular, I would like to discuss 7T° production in pp interactions at low energies.

§1. pp at 4.1 GeV/c (Notre-Dame-Tennessee-Oak-Ridge-ANL-Melbourne Collaboration)

The Argonne 12' bubble chamber filled with a 35mol% Ne-H_2 mixture was used for this experiment. The hydrogen filled TST inserted in the chamber has dimensions of 180 cm (L) x 34 cm (IF) xlOcm (77). The liquid mixture gives the radiation length of about 100 cm, yielding a conversion probability per *y* ray of 56%.

To obtain the TI° multiplicity from the scanning information, a subset of a 10,000 frame sample was scanned for events with or without gammas from frames which contain only one event in the TST and none outside. All gammas, except those which obviously do not point to the vertex, are assumed to be associated with the event in the TST.

Figure 1 shows the gamma multiplicity

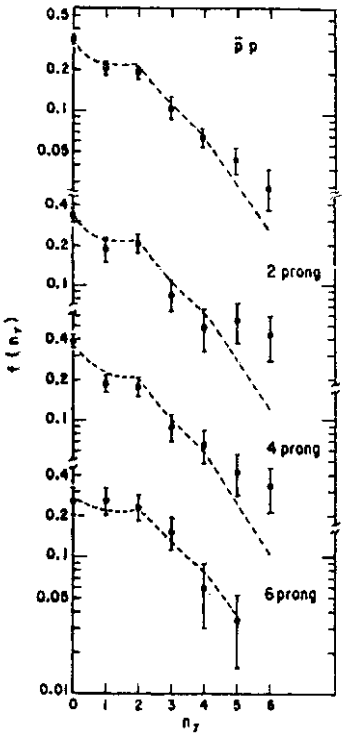

Fig. 1. Frequency $f(n_\gamma)$ as a function of number of γs n_γ for all pp, 2-, 4-, and 6-prong events from the 4.1 GeV/c data.

distributions for all, 2, 4, and 6 prong events. The observed *y* distribution, $f_n(n_\gamma)$, is related to the multiplicity distribution of **7r**°, $g_n(n_\pi)$, by an expression,

(1)

where n_γ, n_π, and n_r are, respectively, the numbers of charged prongs, 7r°'s and ;-'s and *p* is the T* detection efficiency. Since the fitting of

eq. (1) to the *j* multiplicity distribution is not strongly constrained, the TT' multiplicity, $g_n(n_0)$, is chosen to be a sum of two Poisson distributions. The best fit gives $<n_0>=1.41\pm0.07$ with 0.56 where *p* is treated as a free parameter. The results of semi-inclusive ^° production are summarized in Table I.

Table I. Average T T ° multiplicity in pp.

Prong No.	At rest	4.1 GeV/c
0	3.9±0.7	0.96±0.23
2	2.5±0.4	1.35±0.13
4	. . . . .	1.28±0.12
6	.....	1.58±0.16
8		1.11±0.35

The inclusive *n*° cross section is obtained to be o**(7r**°)=74.3±6 mb using an inelastic cross section of 50.2 mb for pp interactions at 4.1 GeV/c. Figure 2(a) shows *a(7t°)* as a function of P_{Lab} for pp and pp interactions. Inclusive cross sections, C7(TT) and (/(^°), in pp annihilations are calculated from the difference of pp and pp cross sections and are plotted in Fig. 2(b). The data points at 4.1 *GeV/c* follow the trend of the energy dependence shown by other experiments. The ratio <J(TT')/ *G(TC°)* is about 2 in this energy range which is J expected from isospin arguments.

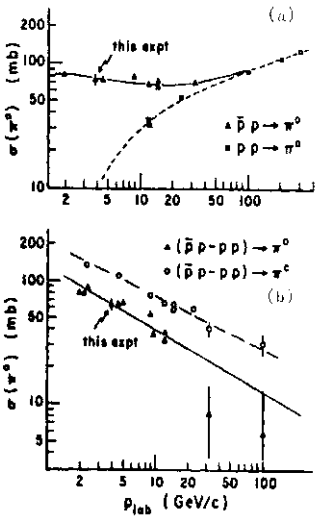

Fig. 2. (a) Inclusive 7r° production cross section for pp and pp interactions as a function of lab momentum, (b) Annihilation *x*° and *n*° cross sections as a function of lab momentum.

§2. pp at Rest (Tohoku University)

A stopping pp experiment was performed using the ANL 12' bubble chamber with the TST to study TT° production in pp annihilations at rest. An 800 MeV/c p beam was reduced by a 12' thick polyethylene degreader to make the p stop at the end of the TST. This degrader also produces background p's.

About 80,000 and 20,000 frames are scanned for 0- and 2-prong events with or without gammas, respectively. These events are measured and processed by the ANL version of TVGP with a modification for the TST optics. Gamma association to a primary vertex was examined by using the momentum direction of the gamma whether the direction point to the vertex. The selection of gammas using the direction criterion reduces the background gammas, but also some of the truely associated gammas.

To obtain the *n*° multiplicity, both /--multiplicity and missing mass distributions are used for the fitting with the binominal equation (1). The use of the missing mass gives additional constraints in fitting. The best fits

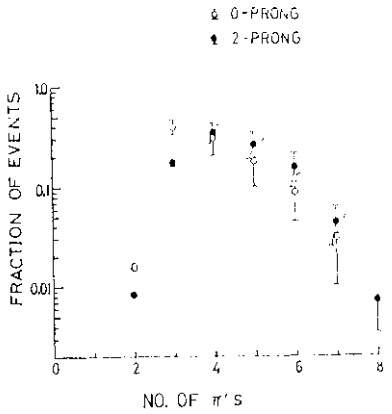

Fig. 3. Total *n* (charged plus neutral *it)* multiplicity distribution for pp annihilations at rest.

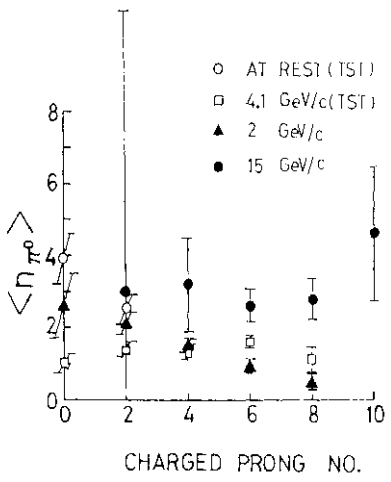

Fig. 4. Average *TC°* multiplicity as a function of charged prong number.

give $\langle\Delta_0\rangle$=-3.9±0.7 and $\langle\alpha_{sc0}\rangle$=2.5±0.4 for the 0- and 2-prong samples. The results are also given in Table I. Figure 3 shows the total π(charged+neutral) multiplicity distributions for the 0- and 2-prong samples. A remarkable similarity is observed between the 0- and 2-prong samples.

Figure 4 shows the average π^0 multiplicity for each charged multiplicity, and a comparison with other experimental data.[1,2] For $n_c>2$, the $\langle w_n\rangle$ seems to be same in this energy region except the 15GeV/c data.[1] There is some discrepancy of $\langle w_0\rangle$ for zero prong events among these experiments. It is not clear whether the discrepancy can be attributed to the difference of the antiproton beam momenta for these experiments.

References

1. T. Kitagaki *et al:* Proceedings, Symposium on Antinucleon-Nucleon Interactions, Liblice, Prague (1974) p. 269.
2. B.S. Chandhary *et al: ibid.,* (1974) p. 163.

Session A4: Low Energy Photoproduction

Chairman: T. FUJII

Organizer: R. KAJIKAWA

Scientific Secretaries: K. UKAI
N. TOKUDA

1. Summary of Low Energy Photoproduction
   R. KAJIKAWA
2. Phenomenological Analysis, etc.
   P. NOELLE
3. Di-Baryon Resonance in *y-d* Collisions
   T. KAMAE
4. π^0-Photoproduction and 5y-Electroproduction at Bonn
   G. H. KNOP

(Thursday, August 24, 1978; 16: 10-17: 20)